Science of the Total Environment xxx (xxxx) xxx

Contents lists available at ScienceDirect

Science of the Total Environment

journal homepage: www.elsevier.com/locate/scitotenv

Biochemical and histopathological impacts of rutile and anatase (TiO_2 forms) in *Mytilus galloprovincialis*

Carla Leite [a], Francesca Coppola [a], Rui Monteiro [b,f], Tania Russo [c], Gianluca Polese [c], Mirtha A.O. Lourenço [d,e], Mariana R.F. Silva [d], Paula Ferreira [d], Amadeu M.V.M. Soares [a], Rosa Freitas [a,*], Eduarda Pereira [b]

[a] Departamento de Biologia & CESAM, Universidade de Aveiro, 3810-193 Aveiro, Portugal
[b] Departamento de Química, CESAM & LAQV-REQUIMTE, Universidade de Aveiro, 3810-193 Aveiro, Portugal
[c] Dipartimento di Biologia, Universitá degli studi di Napoli Federico II, 80126 Napoli, Italy
[d] Departamento de Engenharia de Materiais e Cerâmica, CICECO-Aveiro Instituto de Materiais, Universidade de Aveiro, 3810-193 Aveiro, Portugal
[e] Istituto Italiano di Tecnologia, Center for Sustainable Future Technologies, Via Livorno, 60, 10144 Torino, TO, Italy
[f] CIIMAR, Universidade do Porto, 4450-208, Matosinhos, Portugal

HIGHLIGHTS

- *Mytilus galloprovincialis* bioaccumulated titanium regardless the TiO_2 form.
- Both forms of TiO_2 induced histopathological alterations in mussels.
- Higher oxidative stress was observed in mussels exposed to anatase.
- Neurotoxicity was induced by both forms of TiO_2.

GRAPHICAL ABSTRACT

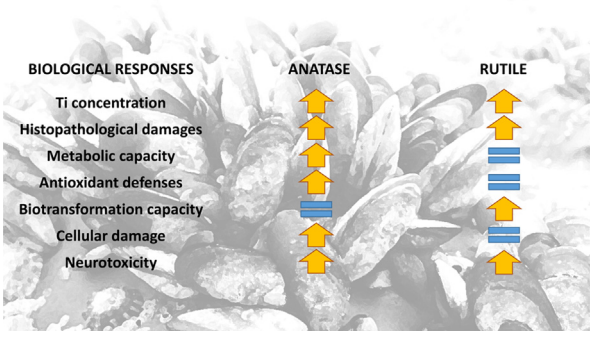

ARTICLE INFO

Article history:
Received 20 July 2019
Received in revised form 6 October 2019
Accepted 6 October 2019
Available online xxxx

Editor: Damia Barcelo

Keywords:
Mussels
Rutile
Anatase
Oxidative stress
Metabolism
Histopathology

ABSTRACT

Titanium dioxide (TiO_2) particles have been widely used in various industrial applications and consumer products. Due to their large production and use, they will eventually enter into aquatic environments. Once in the aquatic environment TiO_2 particles may interact with the organisms and induce toxic effects. Since the most common crystallographic forms of TiO_2 are rutile and anatase, the present study evaluated the effect of these two forms of TiO_2 particles in *Mytilus galloprovincialis*. For this, mussels were exposed to different concentrations of rutile and anatase particles (0, 5, 50, 100 μg/L) for twenty-eight days. Ti concentrations, histopathological alterations and biochemical effects were evaluated. Similar Ti concentrations were found in mussels exposed to rutile and anatase, with the highest values in mussels exposed to the highest exposure concentration. Histopathological results demonstrated that both forms of TiO_2 induced alterations on gills and digestive glands along the increasing exposure gradient. Biochemical markers showed that mussels exposed to rutile maintained their metabolic capacity (assessed by the activity of the Electron Transport System, ETS), while anatase increased the metabolism of mussels. Mussels exposed to rutile increased their detoxifying defences which, due to the low tested concentrations, were sufficient to avoid cellular damage. On the other hand, mussels exposed to anatase suffered cellular damages despite the increase of the antioxidant defences which may be related to the high ETS activity. Both rutile and anatase particles were toxic to *M. galloprovincialis*, being the highest oxidative stress exerted by the crystalline form anatase.

* Corresponding author at: Departamento de Biologia, Universidade de Aveiro, Campus Universitário de Santiago, 3810-193 Aveiro, Portugal.
E-mail address: rosafreitas@ua.pt (R. Freitas).

https://doi.org/10.1016/j.scitotenv.2019.134886
0048-9697/

1. Introduction

Among anthropogenic contaminants of emerging concern are engineered nanomaterials (ENMs) that can be divided into two general classes: carbon-based and metal-containing ENMS (Fadeel and Garcia-Bennett, 2010). Titanium dioxide (TiO_2) are metal oxide particles which are extensively used in various industrial applications and consumer products including water treatment approaches, biomaterials, cosmetics, and electronic equipments (Robichaud et al., 2009; Mezni et al., 2018), mainly due to their high transparency to visible light and high UV absorption (Braydich-Stolle et al., 2009). For this reason it is estimated that the worldwide TiO_2 particles production will reach 2.5 million tons by 2025 (Mezni et al., 2018). There are three crystalline forms of TiO_2: i) anatase (tetragonal), ii) rutile (tetragonal), and iii) brookite (orthorhombic) (Cho et al., 2013; Iswarya et al., 2018). Among these, rutile and anatase are the most common forms of TiO_2 due to their properties such as high photocatalysis and refractive index (Iswarya et al., 2018). Brookite has rarely been used or studied thus far, due to its scarcity in the environment (Allen et al., 2010) and difficulties in preparing significant amounts of good quality material (Gong and Selloni, 2007). Both rutile and anatase forms are widely employed in consumer products like toothpaste, sunscreens, food, paints, plastics, paper, and biomedical devices (Wang et al., 2007; Yang et al., 2009; Middlemas et al., 2013; de la Calle et al., 2017; Barbosa et al., 2018; Leong and Oh, 2018; Dorier et al., 2019). Furthermore, they are also used in environmental oriented applications including wastewater treatment (Yuzer et al., 2015), air purification (Paz, 2010) and soil remediation (Yang and Xing, 2009). Rutile is used in optical elements and as a dielectric material in ceramics (Amtout and Leonelli, 1995; Wang et al., 2019). Anatase is applied as a catalytic support for the production of nanotubes and nanoribbons (Mogilevsky et al., 2008) and used in photovoltaics (Grätzel, 2001). Due to its worldwide production and usage, both forms of TiO_2 particles are released in enormous quantities in urban and industrial sewage and, consequently, reach aquatic environments (Gottschalk and Nowack, 2011; Nowack et al., 2012).

Since estuaries are semi-enclosed coastal bodies of water that connect terrestrial, freshwater and marine systems (Dame, 2008), they are expected to be the ultimate sink for contaminants such as ENMS (Islam and Tanaka, 2004; Dauvin and Ruellet, 2009; Canesi et al., 2010; Barmo et al., 2013). Among these contaminants Ti has been identified in marine systems with concentrations ranging between 0.01 and 5.5 μg/L (Yan et al., 1991; Yokoi and van den Berg, 1991; Skrabal, 2006). With the increased use of TiO_2 and low capacity of wastewater treatment plants to eliminate these particles (Shi et al., 2016), Ti has been detected at concentrations ranging between 100 and 3000 μg/L in sewage (Kiser et al., 2009), and increasing concentrations of Ti in aquatic systems ranging from 5 to 600 μg/L (Kaegi et al., 2008; Menard et al., 2011).

Once in the aquatic environment TiO_2 particles may interact with organisms and induce toxic effects (Iswarya et al., 2019). Previous studies demonstrated that these particles caused severe toxicity towards aquatic organisms. Barmo et al. (2013) showed that TiO_2 affected mussels immune system and digestive gland functioning. Other studies showed the impacts of different forms of TiO_2. Braydich-Stolle et al. (2009) observed that rutile particles were capable of initiating apoptosis, while anatase particles triggered cell necrosis in mouse keratinocytes. Also, Iswarya et al. (2015) demonstrated that rutile and anatase particles caused damage in different parts of the green algae *Chlorella* sp. Rutile caused damages in chloroplast and internal organelles while anatase particles led to nucleus and cell membrane damages. Nevertheless, information on the impacts of these two forms of TiO_2 particles on aquatic species, and especially marine and estuarine organisms, is still limited. Therefore, it is of utmost relevance to understand the impacts of rutile and anatase particles on aquatic environments, namely on inhabiting organisms.

Mytilus galloprovincialis is considered a good bioindicator due to its capacity to tolerate and accumulate various contaminants, sedentary lifestyle, wide geographical distribution and abundance (Wang et al., 1996; Viarengo et al., 2007; Banni et al., 2014). Although recent studies already revealed the impacts of TiO_2 particles in *M. galloprovincialis* (Canesi et al., 2010, 2012; Ciacci et al., 2012; Barmo et al., 2013; Mezni et al., 2018), to our knowledge no information is available on the toxic effects of rutile and anatase forms on this mussel species. Therefore, the present study evaluated the impacts induced by different concentrations of rutile and anatase particles in *M. galloprovincialis*, by measuring histopathological and metabolic alterations as well as oxidative and neurotoxic status.

2. Methodologies

2.1. Anatase and rutile particles characterization

Two commercial TiO_2 particles of different morphology were tested in the present study: i) the rutile form acquired from Alfa Aesar (99.5%), and ii) the anatase form, acquired from Merck (99.7%). The structural and microstructural characterization of rutile and anatase particles were performed by X-ray diffraction (XRD), Raman spectroscopy and scanning electron microscopy (SEM) techniques. The textural properties of the samples were assessed by −196 °C N_2 adsorption-–desorption isotherms. XRD data were collected with a Phillips X'Pert MPD diffractometer using Cu-Kα radiation. The Raman spectra were recorded on a Bruker RFS 100/S FT Raman spectrometer using a 1064 nm excitation of the Nd/YAG laser. SEM images were acquired on a SEM-FEG Hitachi SU-70 microscope operated at 15 kV. Nitrogen adsorption-desorption isotherms were recorded at −196 °C using a Gemini V 2.00 instrument model 2380. The samples were dehydrated overnight at 200 °C to an ultimate pressure of 1024 mbar and then cooled to room temperature prior to adsorption.

The characterization of particles in the exposure medium was made by Dynamic Light Scattering (DLS) analysis. The DLS measurements were carried out using a Nano ZetaSizer, Malvern equipment with a "red" laser operating at 633 nm and a detector positioned at 173 ° at room temperature.

2.2. Sampling and experimental conditions

Mytilus galloprovincialis specimens were collected in September 2018 during low tide in the Ria de Aveiro estuary (northwest coast of Portugal). Mussels were transported to the laboratory, where they were maintained for fifteen days in aquaria for depuration and acclimation to laboratory conditions. During this period, mussels were kept under continuous aeration during a 12 h light: 12 h dark photoperiod and were in synthetic seawater (salinity 30 ± 1, Temperature 18.0 ± 1.0 °C; pH 8.0 ± 0.1), prepared with reverse osmosis water with commercial salt (Tropic Marin® SEA SALT). Seawater was renewed every day in the first three days and every three days until the end of this period and mussels were fed with Algamac protein plus (150,000 cells/animal) three times per week.

During the experimental exposure (twenty-eight days), mussels were distributed into different aquaria with 3 L of synthetic seawater, with five individuals per aquarium and three aquaria per condition. Each aquarium had a diffuser stone for aeration and agitation of the water. Light, salinity, temperature and pH condi-

Please cite this article as: C. Leite, F. Coppola, R. Monteiro et al., Biochemical and histopathological impacts of rutile and anatase (TiO_2 forms) in *Mytilus galloprovincialis*, Science of the Total Environment, https://doi.org/10.1016/j.scitotenv.2019.134886

tions were the same as those used during depuration and acclimation. Mussels were exposed to TiO_2 particles with two different crystallographic forms: rutile and anatase. The concentrations in Ti tested were: CTL) 0 μg/L; C1) 5 μg/L; C2) 50 μg/L; and C3) 100 μg/L. This range of Ti concentrations was selected according to the values reported in previous works for pristine and contaminated aquatic systems (Kennedy et al., 1974; Menard et al., 2011; Shi et al., 2016). For the exposure assay, TiO_2 particles (rutile and anatase) in powder form were dispersed in ultrapure water using a bath sonicator (60 Hz) during 10 min to obtain stock solution of 60 and 600 mg/L of Ti. From these dispersions, appropriate contamination solutions were prepared so that the intended contaminated levels in aquaria were achieved.

During the entire experimental period organisms were fed with Algamac protein plus (150,000 cells/animal) three times a week. Seawater was renewed once a week and Ti solutions were added to the medium immediately after sonication during 5 min. Immediately after the rutile and anatase particles spiking into the water, samples were collected from each aquarium for quantification of Ti in seawater medium.

At the end of the exposure period, with the exception of one mussel per aquarium used for histopathological analyses, the remaining organisms were frozen with liquid nitrogen and stored at −80 °C. Three frozen mussels per aquarium (nine per condition) were homogenized with a mortar and a pestle under liquid nitrogen. Each homogenized organism was divided into 0.5 g fresh weight (FW) aliquots for biomarkers analyses and the remaining tissue was used for Ti quantification.

2.3. Titanium quantification in water and mussel's samples

Total Ti concentrations in waters and *M. galloprovincialis* soft tissues were determined by inductively coupled plasma optical emission spectrometry (ICP-OES), after microwave-assisted acid digestion (CEM MARS 5). Water samples were stirred and then sonicated using a bath sonicator for 10 min to ensure proper dispersion of the potentially present TiO_2 particles. 4 mL of sample, 0.5 mL HNO_3, 0.1 mL HF and 5.4 mL of water sample were added to Teflon tubes. Samples were digested in the microwave by increasing temperature to 180 °C in 10 min, which was then maintained for 10 min. After cooling down, the samples were analysed by ICP-OES. Quality control was kept by blank analysis (reagent mixture), which was below quantification limit (2 μg/L).

Freeze-dried samples (0.2 g) were homogenized and weighted into a Teflon vessel to which 1 mL HNO_3 65%, 1 mL HF 40% and 2 mL H_2O_2 30%, all v/v, were added. Samples were digested in the microwave by increasing temperature to 180 °C in 10 min, which was then maintained for 10 min. After cooling, samples were transferred to polyethylene vessels, made to a final volume of 25 mL with ultrapure water. Quality control was made through the use of blanks (reaction vessels with only reagent mixture), certified reference material BCR-060 (Aquatic Plant, Lagarosiphon major) and duplicates. Blanks samples were always below the quantification limits for Ti (0.25 mg/kg), the coefficient of variation of samples duplicates varied from 1% to 16% and mean percentage of recovery for BCR-060 was 79 ± 2%.

2.4. Histopathological measurements

After the exposure period, one mussel per aquarium was fixed in Bouin's solution (5% of acetic acid, 9% of formaldehyde, 0.9% of picric acid) for 24 h, at 4 °C. Then, samples were kept for a month in 70–75% ethanol, which was changed daily. After this process, a transverse histological sample of approximately 1 cm thickness of the anterior part of each organism was cut and samples were dehydrated in ethanol and placed in xylene. Afterwards, samples were embedded in paraffin (58 °C) in a vacuum stove (D'Aniello et al., 2016; Polese et al., 2016; Zupo et al., 2019). Histological sections of 7 μm thick were cut with a microtome and placed on slides covered with glycerin/albumin. For histological staining, the samples were placed in xylene and rehydrated in ethanol to remove the paraffin. Then, half of the sections were stained with hematoxylin to assess tissue health (Polese et al., 2016; Zupo et al., 2019). The other half of sections were stained with toluidine blue (0.2% of toluidine blue in sodium acetate buffer) to assess the abundance of hemocytes (Gabe, 1968).

Histopathological changes were identified in gills and digestive glands of mussels, in each condition. The histopathological condition index (I_h) was assessed for gills and digestive glands, according to Bernet et al. (1999) and adaptations performed by Costa et al. (2013). The I_h was calculated following the formula:

$$I_h = \frac{\sum_1^j w_j a_{jh}}{\sum_1^j M_j}$$

where I_h is the histophatological index for the individual h; w_j the weight of the j_{th} histopathological alteration; a_{jh} the score attributed to the h_{th} individual for the j_{th} alteration and M_j is the maximum attributable value for the j_{th} alteration. The I_h was determined following the concepts of the differential biological significance of each surveyed alteration (weight) and its degree of dissemination (score). The weights proposed were based on Costa et al. (2013) and ranges between 1 (minimum severity) and 3 (maximum severity) while the score ranges between 0 (none) and 6 (diffuse).

2.5. Biochemical parameters

With the purpose of evaluating the biochemical alterations induced in mussels after exposure to rutile and anatase concentrations, markers related to metabolic capacity (electron transport system (ETS) activity), energy reserves (glycogen (GLY) content, total protein (PROT) content), oxidative stress (superoxide dismutase (SOD) activity; catalase (CAT) activity; glutathione peroxidase (GPx) activity; glutathione reductase (GRed) activity; glutathione S-transferases (GSTs) activity; lipid peroxidation (LPO) levels; protein carbonylation (PC) levels), and neurotoxicity (acetylcholinesterase (AChE) activity) were analysed. To guarantee the validity of the results, the determination of the biochemical parameters was done in duplicate. For each biomarker, the extraction was performed with specific buffers using a proportion of 1:2 (w/v) with the homogenized tissue (Almeida et al., 2015; Coppola et al., 2017; Pinto et al., 2019). Samples were homogenized using a TissueLyser II (Qiagen) for 90 s, after which they were centrifuged for 20 min at 10,000 g (3000 g for ETS) and 4 °C. Supernatants were stored at −80 °C or immediately used.

2.5.1. Metabolic capacity and energy reserves

The ETS activity was measured using the method of King and Packard (1975) with alterations implemented by De Coen and Janssen (1997). Absorbance was determined at 490 nm during 10 min with intervals of 25 s. The amount of formazan formed was calculated using the extinction coefficient (ε) 15,900 $(mmol/L)^{-1}$ cm^{-1}. The results were expressed in nmol per min per g FW.

The GLY content was evaluated following the sulfuric acid method (Dubois et al., 1956), using glucose standards between 0 and 10 mg/mL to obtain a calibration curve. Absorbance was measured at 492 nm and the results were expressed in mg per g FW.

For PROT quantification the spectrophotometric Biuret method was used, as described by Robinson and Hodgen (1940). Bovine serum albumin (BSA) was applied to prepare standard solutions in the range 0 – 40 mg/mL to obtain a calibration curve. The absor-

Please cite this article as: C. Leite, F. Coppola, R. Monteiro et al., Biochemical and histopathological impacts of rutile and anatase (TiO_2 forms) in *Mytilus galloprovincialis*, Science of the Total Environment, https://doi.org/10.1016/j.scitotenv.2019.134886

bance was measured at 540 nm and results were expressed in mg per g FW.

2.5.2. Antioxidant and biotransformation defenses

The activity of SOD was quantified based on the method described by Beauchamp and Fridovich (1971) with modifications implemented by Carregosa et al. (2014). SOD standards in the range 0.25 – 60 U/mL were used in order to obtain a calibration curve. Absorbance was read at 560 nm and the activity was expressed in U per g FW, where one unit (U) represents the amount of the enzyme that catalyses the conversion of 1 μmol of substrate per min.

The activity of CAT was determined following Johansson and Borg (1988). Formaldehyde standards between 0 and 150 μmol/L were used in order to obtain a calibration curve. Absorbance was measured at 540 nm and the activity was expressed in U per g FW, where U represents the amount of enzyme that caused the formation of 1.0 nmol formaldehyde per min.

The activity of GPx was evaluated using the method of Paglia and Valentine (1967). Absorbance was measured at 340 nm during 5 min in 10 s intervals. The activity was determined using the extinction coefficient (ε) 6.22 $(mmol/L)^{-1}$ cm^{-1}. Activity was expressed in U per g FW, where U corresponds to the quantity of enzyme that caused the formation of 1.0 μmol NADPH oxidized per min.

The activity of GRed was quantified following the method described by Carlberg and Mannervik (1985). Absorbance was measured at 340 nm and the activity was determined using the extinction coefficient (ε) 6.22 $(mmol/L)^{-1}$ cm^{-1}. The activity was expressed in U per g FW, where U represent the amount of enzyme that caused the formation of 1.0 μmol NADPH oxidized per min.

The activity of GSTs was quantified based on the technique of Habig et al. (1974) with adaptations performed by Carregosa et al. (2014). Absorbance was measured at 340 nm during 5 min in 10 s intervals. The amount of thioether formed was calculated using the extinction coefficient (ε) 9.6 $(mmol/L)^{-1}$ cm^{-1}. The activity was expressed in U per g FW, where U represents the quantity of enzyme that causes the formation of 1 μmol of dinitrophenyl thioether per min.

2.5.3. Cellular damage

Levels of LPO were quantified by the measurement of malondialdehyde (MDA) content, following the method described by Ohkawa et al. (1979). Absorbance was measured at 535 nm and the amount of MDA formed was calculated using the extinction coefficient (ε) 156 $(mmol/L)^{-1}$ cm^{-1}. The results were expressed in nmol per g FW.

Levels of PC were determined using the DNPH alkaline method described by Mesquita et al. (2014). Absorbance was measured at 450 nm and PC levels were determined using the extinction coefficient (ε) 0.022 $(mmol/L)^{-1}$ cm^{-1}. The results were expressed in nmol of protein carbonyls groups formed per g FW.

2.5.4. Neurotoxicity

The activity of AChE was assessed using acetylthiocholine iodide (ATChI, 5 mmol/L) substrates, according to the method of Ellman et al. (1961) with alterations performed by Mennillo et al. (2017). The activity of AChE was measured at 412 nm during 5 min and expressed in nmol per min per g FW using the extinction coefficient (ε) 13.6×10^3 $(mol/L)^{-1}$ cm^{-1}.

2.6. Statistical analyses

Results on Ti concentrations, histopathological indexes (I_h for gills and digestive tubules) and biochemical markers (ETS, PROT, GLY, SOD, CAT, GPx, GRed, GSTs, LPO, PC and AChE) obtained for mussels exposed to different conditions were submitted to a statistical hypothesis testing using permutational analysis of variance, employing the PERMANOVA + add-on in PRIMER v6 (Anderson et al., 2008). The pseudo-F *p*-values in the PERMANOVA main tests were evaluated in terms of significance. When significant differences were observed in the main test, pairwise comparisons were performed. Values lower than 0.05 ($p < 0.05$) were considered as significantly different. The null hypotheses tested were: i) for each biological response (Ti accumulation in soft tissues, histopathological and biochemical markers), and TiO_2 particles (rutile or anatase), no significant differences existed among exposure concentrations (0, 5, 50 and 100 μg/L), with significant differences represented in figures with different lowercase letters for rutile particles and uppercase letter for anatase particles; ii) for each biological response (Ti accumulation in soft tissues, histopathological and biochemical markers) and Ti exposure concentration (0, 5, 50 and 100 μg/L), no significant differences existed between TiO_2 particles (rutile and anatase), with significant differences represented in figures with an asterisk.

The matrix gathering the biological responses (histopathological and biochemical markers) and Ti concentrations in mussel tissues for each condition were used to calculate the Euclidean distance similarity matrix. This similarity matrix was simplified through the calculation of the distance among centroids matrix based on the exposure condition, which was then submitted to ordination analysis, performed by Principal Coordinates (PCO). Pearson correlation vectors of biochemical descriptors, histopathological indices and Ti concentration (correlation >0.75) were provided as supplementary variables being superimposed on the top of the PCO graph.

3. Results

3.1. Anatase and rutile particles characterization

The physical and textural properties of both anatase and rutile samples were studied by XRD, Raman, SEM and −196 °C N_2 adsorption-desorption isotherms. XRD diffractograms (Fig. 1S, Supplementary Materials, SM) verified that both samples were monophasic presenting the most representative reflections of rutile (JCPDS no. 04-013-6225) and anatase (JCPDS no. 016-2837), confirming the presence of rutile ($P\frac{4_2}{m}$nm) and anatase ($I\frac{4}{a}$md) tetragonal phases. The rutile lattice constants were $a = b = 4.5922$ and $c = 2.9578$ Å. The anatase lattice parameters were $a = b = 3.7924$ and $c = 9.5304$ Å. The densities of the rutile and anatase particles were calculated from the lattice parameters as 3.38 and 4.27 g/cm^3, respectively. Raman spectroscopy displayed at Fig. 2S also confirmed the characteristic vibrational modes of the pure crystallographic forms of rutile and anatase. SEM micrographs are shown at Fig. 1. The rutile particles present undefined morphology with aggregates of relatively large size as depicted in the inset of Fig. 1. The anatase particles are small and round shaped with an average diameter of 180 ± 24 nm (resulting from the measurement of 50 particles). As it can be observed, rutile displays bigger particles than anatase. −196 °C N_2 adsorption isotherms were measured for both oxides (not shown) and the specific surface areas (S_{BET}) calculated were 3 and 8 m^2/g for rutile and anatase, respectively. Both particles present low specific surface area probably due to the agglomeration level. The anatase particles have a slightly higher specific surface area than rutile which can be related to the smallest size.

The behaviour of the rutile and anatase particles in suspension in the exposure medium was investigated by DLS. Table 1 resumes the size distribution of the oxide suspensions in the exposure medium along 24 h. The DLS measurements were performed using a

Please cite this article as: C. Leite, F. Coppola, R. Monteiro et al., Biochemical and histopathological impacts of rutile and anatase (TiO_2 forms) in *Mytilus galloprovincialis*, Science of the Total Environment, https://doi.org/10.1016/j.scitotenv.2019.134886

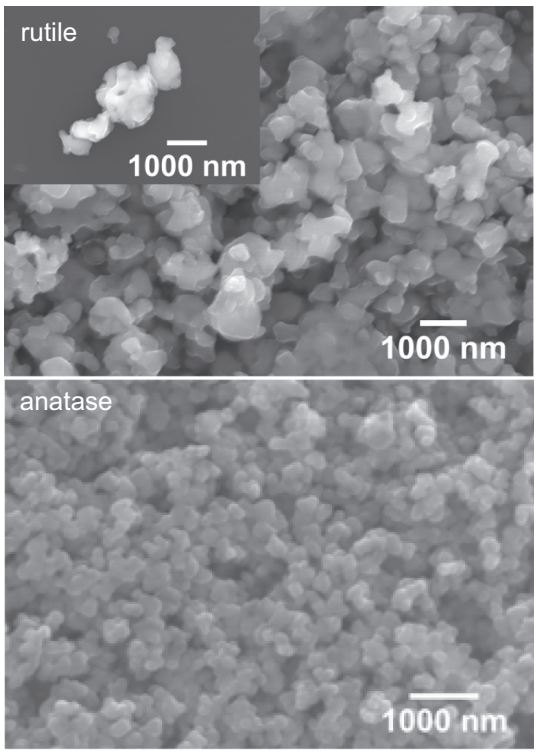

Fig. 1. SEM micrographs illustrating the typical morphology of rutile and anatase particles. The rutile particles present undefined morphology with aggregates of relatively large size as depicted in the inset. The anatase particles are small and round shaped with an average diameter of 180 ± 24 nm (measurement of 50 particles).

Table 1
Z-average size distributions of rutile and anatase particles suspensions with concentration of 100 mg/L in exposure medium as determined by DLS at 25 °C.

Oxide	Z-Average size (nm)		
	After 15 min	After 1 h	After 24 h
Rutile	1659 ± 28	4066 ± 268	2139 ± 71
Anatase	1607 ± 77	3303 ± 337	3560 ± 532

concentration of 100 mg/L, 1000 times superior to the maximum expose to the mussels, in order to be above the resolution of the equipment. The Z-average size distribution values were collected after 15 min, 1 h and 24 h. Both oxides showed a strong tendency to agglomerate within the first hour as particles are not stabilized by the interparticle repulsive forces. After 1 h, the biggest aggregates tend to deposit and only the smallest aggregates are kept in suspension. As it can be observed, anatase suspension is almost stabilised after 1 h and almost does not change till the 24 h measurement. In the case of rutile, at the 1 h the particles are very aggregated displaying a Z-Average size value of 4066 ± 268 nm which decreases to 2139 ± 71 nm by 24 h. This decrease can be associated to the deposition of the biggest particles, leading in suspension just the smallest ones, which should be in very small quantity. It should be emphasised that the last measurement did not fit the quality criteria of the equipment due to the presence of sedimenting particles and low concentration of particles in suspension.

3.2. Titanium concentrations in water and mussel's samples

Ti concentration in water samples was below the detection limit (2 μg/L). The Ti concentration in *M. galloprovincialis* exposed to rutile particles increased along the exposure gradient, with significant differences only at the highest exposure concentration comparatively to the remaining conditions (Table 2). Similarly, Ti concentration in mussels exposed to anatase particles tended to increase along the exposure gradient, with significantly higher values in organisms exposed to 100 μg/L in comparison to the remaining conditions (Table 2). At each exposure concentration, similar Ti concentrations were found in mussels exposed to rutile and anatase (Table 2).

3.3. Histopathological parameters

The exposure to TiO_2 particles at different concentrations led to an increase of damage severity in gills in a dose dependent manner, regardless the TiO_2 form (rutile or anatase) (Fig. 2). In particular, along the increasing exposure gradient, gills of *M. galloprovincialis* exposed to rutile showed a progressive increase of lipofuscin aggregates, enlargement of the central vessel and hemocytes infiltration. Similarly, gills of mussels exposed to anatase showed a progressive increase of lipofuscin aggregates, enlargement of the central vessel, loss of cilia and hemocytes infiltration with the increasing exposure concentration. Regarding the I_h of mussels' gills (Fig. 3A) the values significantly increased along the exposure gradient under both forms of TiO_2 particles, with the highest values at the uppermost tested concentration. No significant differences were observed between rutile and anatase particles for each of the tested concentrations.

Mussels' digestive glands (Fig. 4) showed that exposure to rutile particles lead to an increase accumulation of lipofuscin, atrophy and hemocytes infiltration. In mussels exposed to anatase particles (Fig. 4) an increase of atrophy and hemocytes infiltration was observed and lipofuscin aggregates grow at 5 and 50 μg/L of Ti particles. No necrosis was found at any concentration for both forms of TiO_2 particles. In *M. galloprovincialis* exposed to rutile, the I_h regarding mussels' digestive gland (Fig. 3B) significantly expanded along the exposure gradient, with the highest values at the maximum exposure concentration. The I_h regarding the digestive gland of mussels exposed to anatase was significantly higher in contaminated mussels than in non-contaminated ones. No significant differences were observed between anatase and rutile particles for each of the tested concentrations.

3.4. Biochemical parameters

3.4.1. Metabolic capacity and energy reserves

In terms of ETS values, *M. galloprovincialis* exposed to rutile particles did not differ significantly from non-contaminated mussels. In organisms exposed to anatase, significantly higher ETS values were observed at 50 μg/L of Ti particles than in the control mussels.

Table 2
Concentrations of Ti (μg/g) in mussel's soft tissues after 28 days of exposure to each condition of rutile and anatase forms (CTL, 5, 50 and 100 μg/g of Ti). Significant differences ($p \leq 0.05$) among conditions are represented with different letters (lowercase letters for rutile; uppercase letters for anatase). Significant differences ($p \leq 0.05$) between the two forms of TiO_2 at each exposure concentration were represented with asterisks.

	Exposure conditions	[Ti] (μg/g)
	CTL	$2.1 \pm 0.3^{a,A}$
Rutile	5 μg/L	2.4 ± 1.0^{a}
	50 μg/L	2.5 ± 0.4^{a}
	100 μg/L	4.5 ± 0.3^{b}
Anatase	5 μg/L	2.3 ± 0.8^{A}
	50 μg/L	2.8 ± 0.2^{A}
	100 μg/L	5.3 ± 0.7^{B}

Please cite this article as: C. Leite, F. Coppola, R. Monteiro et al., Biochemical and histopathological impacts of rutile and anatase (TiO_2 forms) in *Mytilus galloprovincialis*, Science of the Total Environment, https://doi.org/10.1016/j.scitotenv.2019.134886

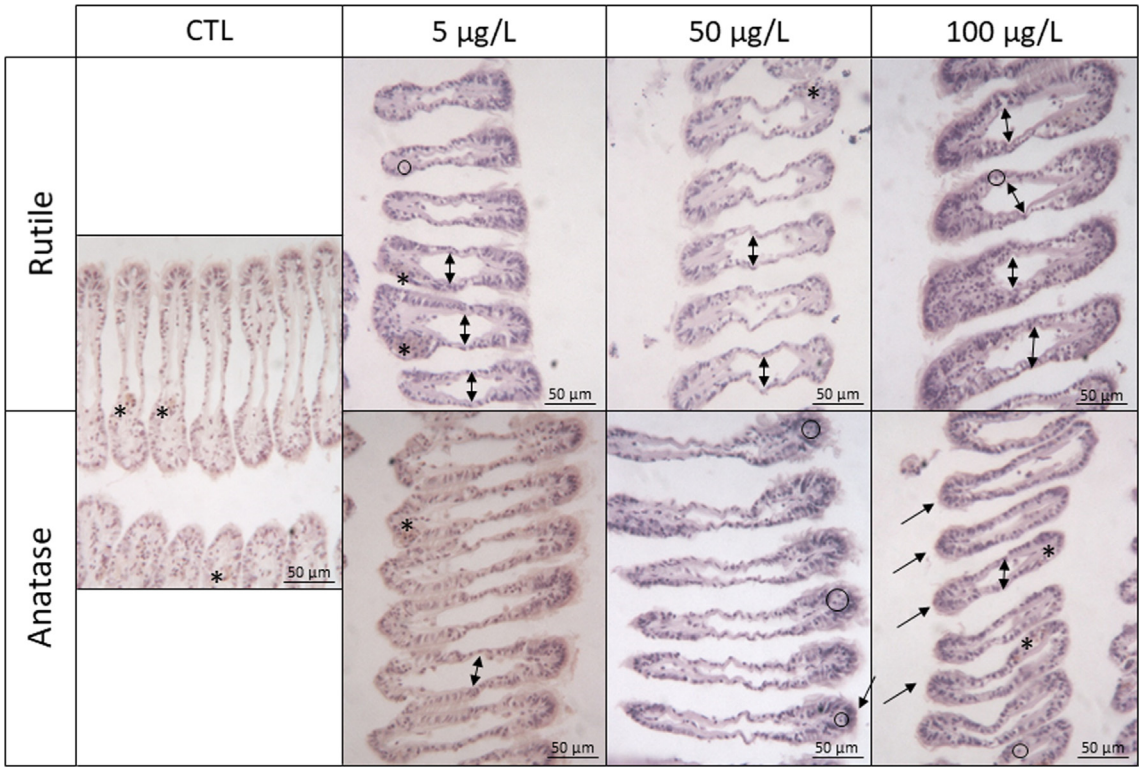

Fig. 2. Micrographs of histopathological alterations observed in the gills of *M. galloprovincialis* exposed to different Ti concentrations of rutile and anatase stained with hematoxylin: lipofuscin aggregates (*); enlargement of the central vessel; hemocytes infiltration (circles) and loss of cilia (arrows). Scale bar = 50 µm.

No significant differences were observed between rutile and anatase particles for each of the tested concentrations (Fig. 5A).

In mussels exposed to both forms of TiO_2 particles the GLY content was significantly higher in contaminated mussels comparatively to non-contaminated ones. No significant differences were observed between the forms of TiO_2 particles tested for each concentration (Fig. 5B).

The PROT content in mussels exposed to rutile particles was lower in contaminated mussels than in non-contaminated ones, with significant differences only between organisms under control and exposed to 5 µg/L of Ti particles. In mussels exposed to anatase, a significantly lower PROT content was showed in organisms exposed to 5 and 100 µg/L of Ti particles in comparison to control organisms and those exposed to 50 µg/L. No significant differences were observed between rutile and anatase particles for each of the tested concentrations (Fig. 5C).

3.4.2. Antioxidant and biotransformation defences

In mussels exposed to rutile particles SOD activity increased at the lowest exposure concentration (5 µg/L) while significantly decreased at 50 and 100 µg/L of Ti particles. The activity of SOD in mussels exposed to anatase particles significantly increased in mussels exposed to 50 µg/L of Ti particles. Comparing both forms of TiO_2 particles, SOD activity was significantly higher in organisms exposed to rutile particles at 5 µg/L while an opposite pattern was observed at 50 µg/L (Fig. 6A).

The activity of CAT showed no significant differences among mussels exposed to rutile particles and non-contaminated mussels. Mussels exposed to anatase particles showed significantly higher CAT activity at 50 µg/L of Ti particles. Differences between rutile and anatase particles were only observed in organisms exposed to 50 µg/L of Ti particles, with the highest activity being in mussels exposed to anatase (Fig. 6B).

Mussels exposed to lower rutile concentrations (5 and 50µg/L of Ti) showed significantly higher GPx activity relatively to non-contaminated mussels. Significantly higher GPx activity was observed in mussels exposed to anatase particles at higher exposure concentrations (50 and 100 µg/L) than others. When relating both forms of TiO_2 particles, significant differences were observed in organisms exposed to 5 µg/L, with the highest activity recorded in mussels exposed to rutile (Fig. 6C).

The activity of GRed in mussels exposed to rutile particles was significantly higher at the lowest exposure concentration (5 µg/L) in contrast to the control mussels and organisms exposed to 50 µg/L. The activity of GRed in mussels exposed to anatase particles was significantly higher at 5 µg/L of Ti particles, comparatively to the remaining conditions. When analysing rutile and anatase particles side by side, significant differences were observed in organisms exposed to 50 µg/L, with the highest activity found in mussels exposed to anatase (Fig. 6D).

The activity of GSTs in mussels exposed to rutile particles was significantly higher at the highest exposure concentration (100 µg/L) than at the other conditions. In mussels exposed to anatase particles GSTs activity significantly decreased at higher exposure concentrations (50 and 100 µg/L) than in mussels in the control group and those exposed to 5 µg/L. When comparing both tested forms of TiO_2 particles, significant differences were observed in organisms exposed to 50 and 100 µg/L, with the highest activity present in mussels exposed rutile (Fig. 7).

3.4.3. Cellular damage

Mussels exposed to rutile particles significantly decreased their LPO levels at the lowest exposure concentration in comparison to mussels under control and those exposed to 50 µg/L. LPO levels were significantly higher in mussels exposed to anatase particles than in non-contaminated mussels. Significant differences between rutile and anatase particles were observed in contami-

Please cite this article as: C. Leite, F. Coppola, R. Monteiro et al., Biochemical and histopathological impacts of rutile and anatase (TiO_2 forms) in *Mytilus galloprovincialis*, Science of the Total Environment, https://doi.org/10.1016/j.scitotenv.2019.134886

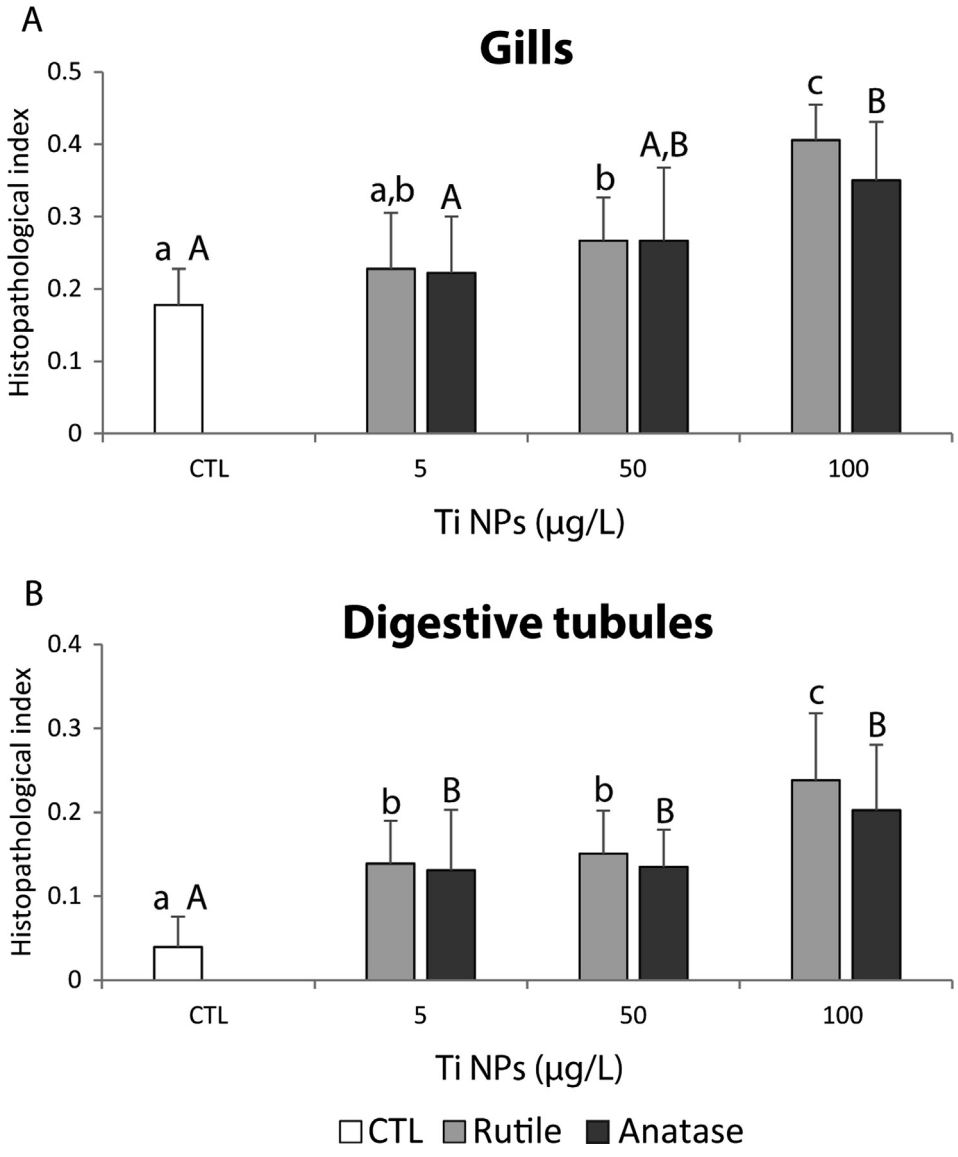

Fig. 3. Histopathological index in A: gills; and B: digestive tubules, in *Mytilus galloprovincialis* exposed to different Ti concentrations of rutile and anatase. Results are mean + standard deviation. Significant differences ($p \leq 0.05$) among conditions are represented with different letters (lowercase letters for rutile; uppercase letters for anatase). Significant differences ($p \leq 0.05$) between the two forms of TiO_2 at each exposure concentration were represented with asterisks.

nated mussels, with the highest values in mussels exposed to anatase (Fig. 8A).

PC levels in mussels exposed to rutile were significantly lower at the lowest exposure concentration and significantly higher at the intermediate exposure concentration in comparison to control and the highest concentration. PC levels in organisms exposed to anatase were significantly lower only at the highest exposure concentration than in the remaining conditions. Comparing both forms of TiO_2 particles, the levels of PC were significantly higher in organisms exposed to anatase at 5 µg/L while an opposite pattern was observed at 50 and 100 µg/L (Fig. 8B), with significantly higher values in organisms exposed to rutile at these concentrations.

3.4.4. Neurotoxicity

In mussels exposed to rutile particles the activity of AChE significantly increased at 50 and 100 µg/L. Mussels exposed to anatase particles showed significantly higher AChE activity than in non-contaminated mussels. Comparing both forms of TiO_2 particles, AChE values were significantly higher in mussels exposed to anatase at 5 µg/L than in rutile (Fig. 9)

3.5. Multivariate analysis

Results from the PCO analysis are presented in Fig. 10. The first principal component axis (PCO1), which represents 32.3% of the variability, clearly separated organisms exposed to control and the lowest Ti particles concentration for both rutile and anatase (positive side) from organisms exposed to higher concentrations (negative side). PCO2 axis explained 24.7% of the variability, separating organisms exposed to the highest rutile concentrations (negative side) from organisms exposed to remaining conditions (positive side). Ti concentration, histopathological indices, GLY and GPx were the variables best correlated with PCO1 negative side ($r > 0.8$), being associated with 100 µg/L of Ti both for rutile and anatase particles. The variables LPO, ETS and SOD were highly correlated with PCO2 positive side ($r > 0.8$), being closely related to 50 µg/L for anatase particles.

Please cite this article as: C. Leite, F. Coppola, R. Monteiro et al., Biochemical and histopathological impacts of rutile and anatase (TiO_2 forms) in *Mytilus galloprovincialis*, Science of the Total Environment, https://doi.org/10.1016/j.scitotenv.2019.134886

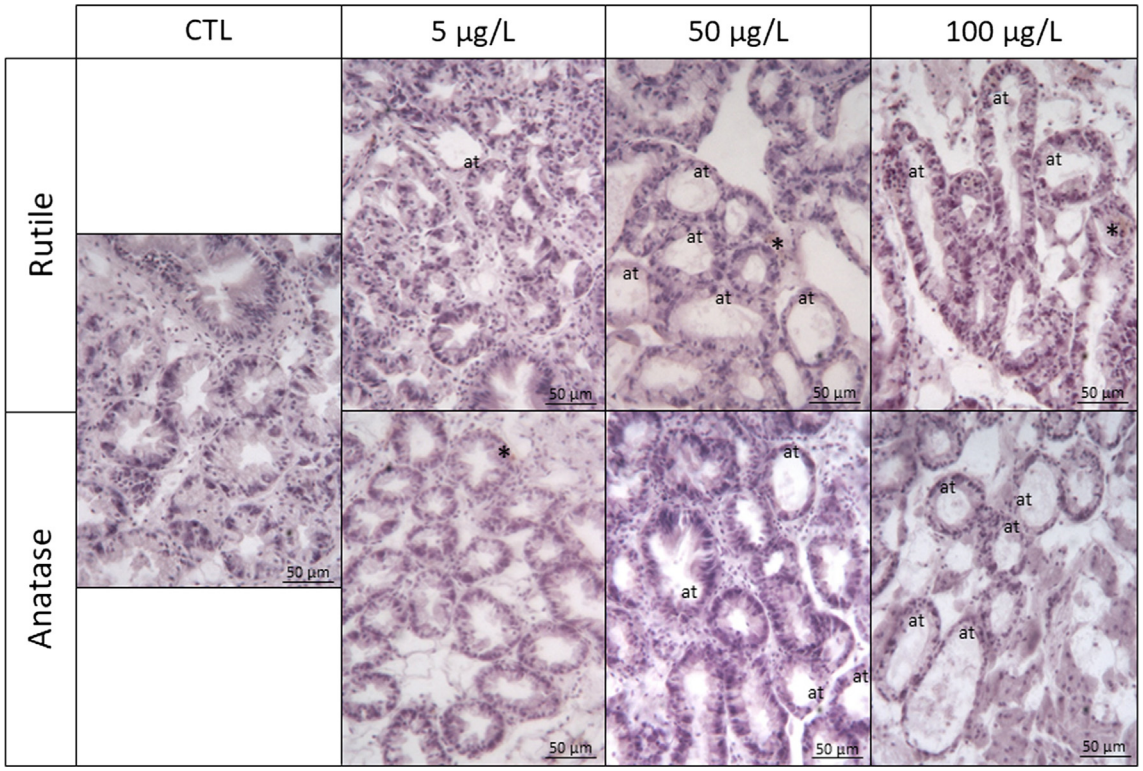

Fig. 4. Micrographs of histopathological alterations observed in the digestive tubules of *M. galloprovincialis* exposed to different Ti concentrations of rutile and anatase stained with hematoxylin: atrophied digestive tubule (at) and lipofuscin accumulation (*). Scale bar = 50 µm.

4. Discussion

The present study evaluated the impacts induced by rutile and anatase particles in the species *M. galloprovincialis* assessing mussels' histopathological alterations and biochemical effects, including impacts on organism's metabolism, energy reserves, oxidative and neurotoxic status. The impacts observed in the present study can be clearly associated with the Ti concentration measured in mussel's soft tissues, which increased along the increasing exposure gradient, with the highest impacts and Ti concentrations in mussel's soft tissues at the highest tested concentration regardless the TiO_2 form (rutile or anatase).

Although, the selected particles were studied by XRD, Raman spectroscopy, and BET analysis in the powder form, the behaviour of them in the experimental medium was expected to be very different. So, to understand the behaviour of rutile and anatase particles in the exposure medium DLS studies over 24 h were performed. The DLS results showed that both forms of TiO_2 particles tended to aggregate in the first contact with the medium. However, after the first hour, the behaviour of the two oxides particles is quite different. In the case of rutile particles, after 1 h the Z-average size is as big as 4066 ± 268 nm decreasing after to 24 h to 2139 ± 71 nm probably because the largest aggregates deposit at the bottom of the aquaria. It was assumed that very low quantity of particles was still suspended in the medium as the DLS measurements report at 24 h lacked quality. This observation evidences the low stability of the rutile particles in the high ionic force medium, which leads to high degree of deposition, and reduces the availability to the mussels. In the case of anatase, the Z-average size was already stabilised after 1 h. Table 1 shows a Z-average size of 3303 ± 337 nm after 1 h, remaining about the same after 24 h (3560 ± 532 nm). This may indicate the faster stabilization of anatase particles relatively to the rutile ones. The anatase particles remained suspended in the exposure medium at least since 1 h after dispersion in the medium in a stable way, which may indicate a higher availability to organisms than rutile. These results are in good agreement with the ones reported by Canesi et al., 2010; Zhu et al., 2011 showing that TiO_2 particles form aggregates in artificial seawater and thus tend to precipitate rapidly to the bottom of the aquarium, and correlating this with the high ionic strength of the seawater. Jiang et al. (2009) justified the observation based on the decrease of the energy barrier to avoid agglomeration with increase of the ionic strength of the medium. Nevertheless, in the present study, mussels accumulated identical amounts of rutile and anatase particles. According to Ciacci et al. (2012) the aggregation increases with increasing concentration and Ward and Kach (2009) demonstrated that bivalves more efficiently capture and ingest particles that are incorporated into agglomerates compared to those freely dispersed. So, the present results may indicate that increasing concentrations may result into larger and/or more aggregates with consequent enhancement of the accumulation and of the toxicity. Based in these authors, a possible justification for similar uptakes of both oxides by the bivalves may be the larger aggregates of rutile (as observed by DLS) in relation to the anatase which may allowed the bivalves to uptake more rutile in a shorter time than in the case of anatase. Anatase particles are more stable, remaining longer available for ingestion by the mussels.

The biological effects of rutile and anatase may be associated to the structure of these particles. Jin et al. (2011) demonstrated that anatase had the ability to induced reactive oxygen species (ROS) generation while rutile particles were not able to induce ROS generation. As observed by XRD and Raman, the particles selected for this study present rutile and anatase crystallographic pure phases. Both structures are tetragonal, consisting of TiO_6 octahedra which share four edges in anatase and two edges in rutile. Anatase is a metastable phase with lower surface energy than rutile and is firstly formed from the assemblage of TiO_6 monomers. Rutile is the most stable phase at all conditions, having the lowest bulk free

Please cite this article as: C. Leite, F. Coppola, R. Monteiro et al., Biochemical and histopathological impacts of rutile and anatase (TiO_2 forms) in *Mytilus galloprovincialis*, Science of the Total Environment, https://doi.org/10.1016/j.scitotenv.2019.134886

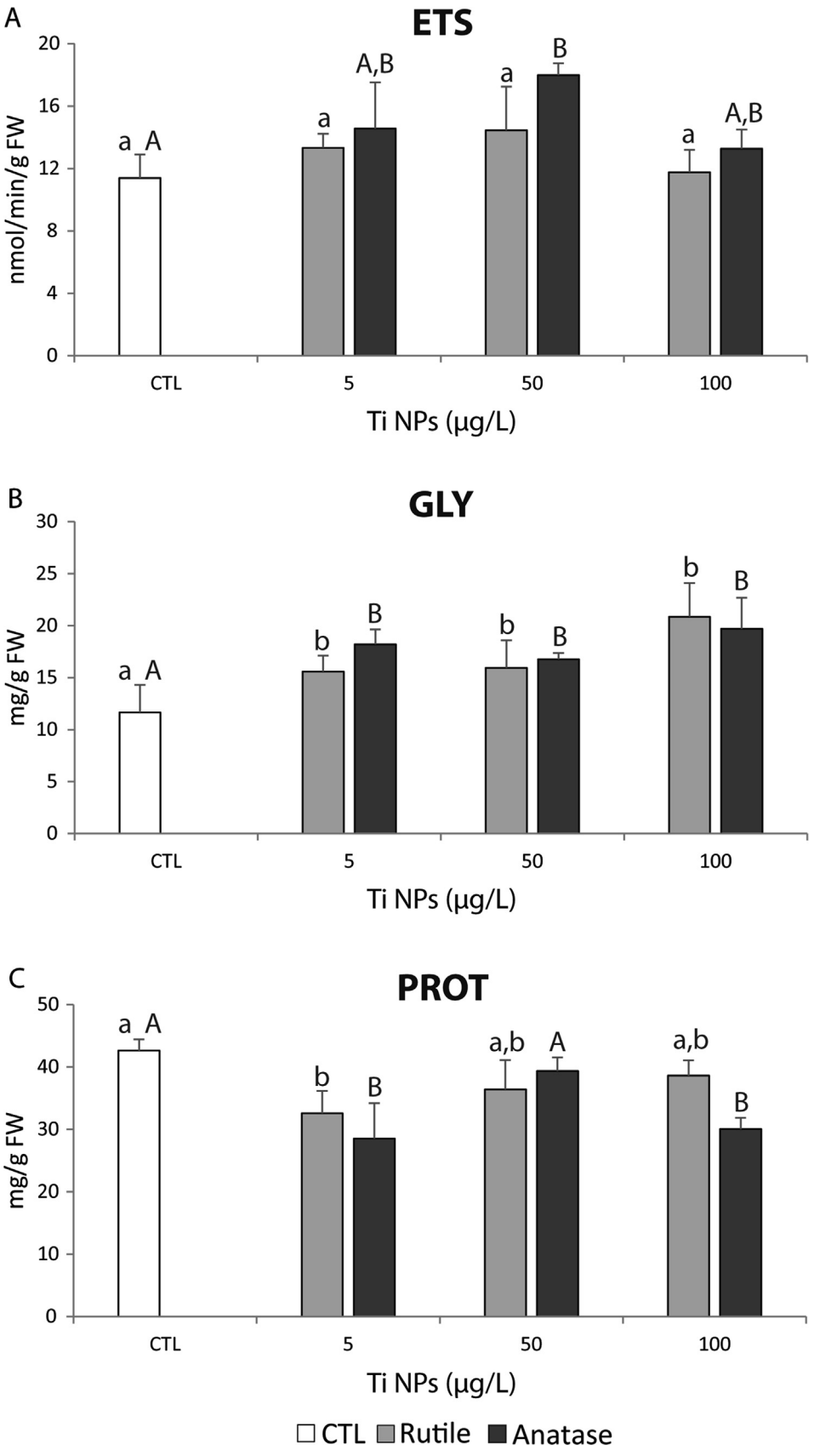

Fig. 5. A: Electron transport system activity (ETS), B: Glycogen content (GLY) and C: Protein content (PROT), in *Mytilus galloprovincialis* exposed to different Ti concentrations of rutile and anatase. Results are mean + standard deviation. Significant differences ($p \leq 0.05$) among conditions are represented with different letters (lowercase letters for rutile; uppercase letters for anatase). Significant differences ($p \leq 0.05$) between the two forms of TiO_2 at each exposure concentration were represented with asterisks.

Please cite this article as: C. Leite, F. Coppola, R. Monteiro et al., Biochemical and histopathological impacts of rutile and anatase (TiO_2 forms) in *Mytilus galloprovincialis*, Science of the Total Environment, https://doi.org/10.1016/j.scitotenv.2019.134886

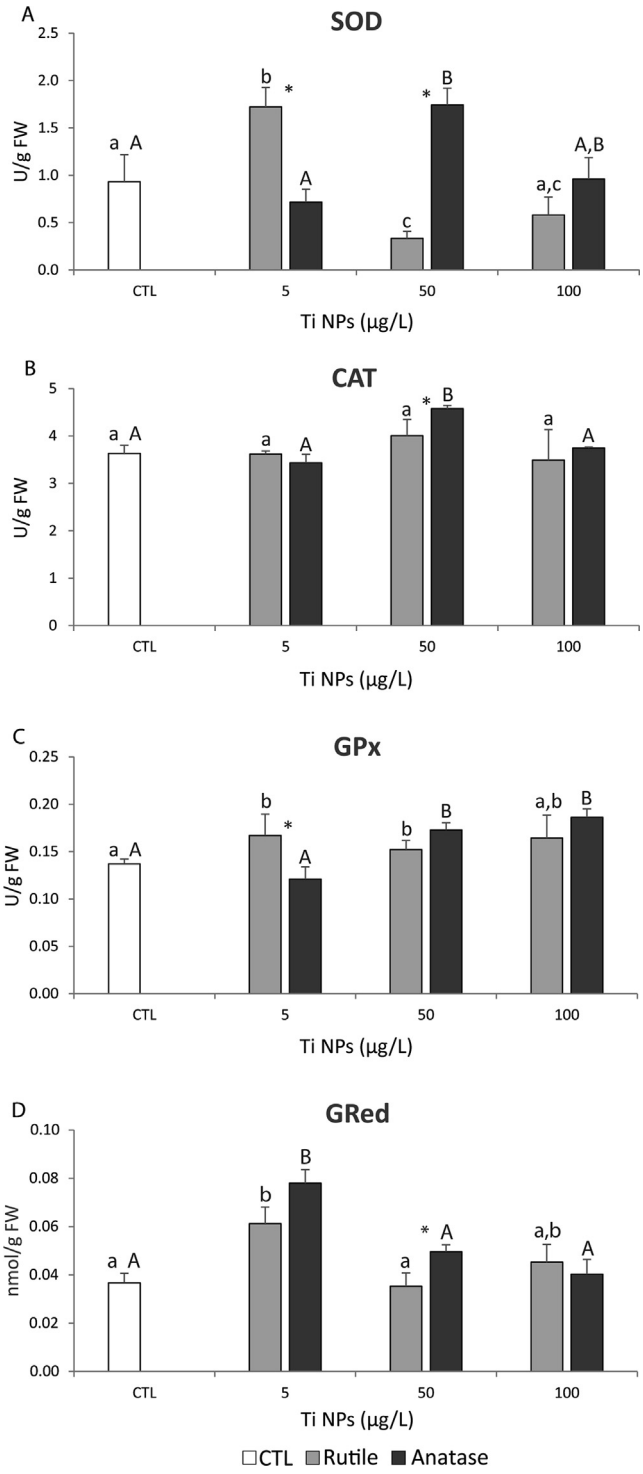

Fig. 6. A: Superoxide dismutase activity (SOD); B: Catalase activity (CAT); C: Glutathione peroxidase activity (GPx); and D: Glutathione reductase activity (GRed), in *Mytilus galloprovincialis* exposed to different Ti concentrations of rutile and anatase. Results are mean + standard deviation. Significant differences ($p \leq 0.05$) among conditions are represented with different letters (lowercase letters for rutile; uppercase letters for anatase). Significant differences ($p \leq 0.05$) between the two forms of TiO_2 at each exposure concentration were represented with asterisks.

energy of the two polymorphs. Typically, anatase is reported to have higher reactivity as a consequence of the highest density of localised states with surface-adsorbed hydroxyl radicals and of the slowest charge carrier recombination compared to rutile (Hanaor and Sorrell, 2011). These characteristic of anatase may suggest that this polymorph is more prompt after being uptaken by the mussels to undergo biological interactions.

In what regards to toxic effects, histopathological observations confirmed that both forms of TiO_2 particles induced alterations in mussels' gills and digestive tubules. Since gills interact with the surrounding environment, they are one of the main target organs for contaminants (Evans, 1987; Au, 2004; Rajalakshmi and Mohandas, 2005). In the present study, the exposure to rutile and anatase particles resulted in an abundance of lipofuscin

Please cite this article as: C. Leite, F. Coppola, R. Monteiro et al., Biochemical and histopathological impacts of rutile and anatase (TiO_2 forms) in *Mytilus galloprovincialis*, Science of the Total Environment, https://doi.org/10.1016/j.scitotenv.2019.134886

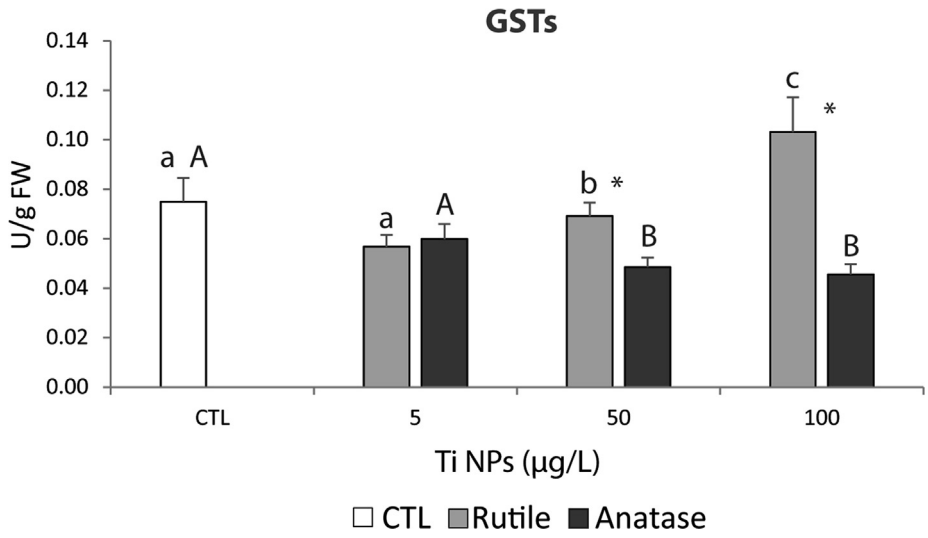

Fig. 7. Glutathione S-transferases activity (GSTs), in *Mytilus galloprovincialis* exposed to different Ti concentrations of rutile and anatase. Results are mean + standard deviation. Significant differences ($p \leq 0.05$) among conditions are represented with different letters (lowercase letters for rutile; uppercase letters for anatase). Significant differences ($p \leq 0.05$) between the two forms of TiO_2 at each exposure concentration were represented with asterisks.

aggregates, hemocyte infiltration and an enlargement of the central vessel. The presence of lipofuscin aggregates was previously associated with oxidative stress in bivalves (Livingstone et al., 2006), which is in accordance with the present results obtained in mussels exposed to anatase particles. However, in mussels exposed to rutile particles the appearance of these aggregates was not accompanied by cellular damage which may indicate the low toxicity of rutile in terms of biochemical changes and, on the other hand, higher responsiveness of mussels in terms of histopathological changes towards this TiO_2 form. In what regards to hemocytes infiltration these alterations are clearly a consequence of mussels' exposure to rutile and anatase particles. Similar alterations were already observed by Bignell et al. (2011) and Amachree et al. (2014) in mussels exposed to other stressful conditions, namely the presence of pathogens and mercury, respectively. The loss of cilia was only observed in mussels exposed to anatase, which may indicate higher toxicity of these particles than the rutile ones. According to Pagano et al. (2016), the loss of cilia may lead to difficulties in filtering food and breathing problems, highlighting possible physiological impairments in mussels exposed to these particles which can compromise mussel's growth and reproduction success. Previous studies conducted by D'Agata et al. (2014) also showed that mussels suffered histopathological alterations in gills due to exposure to 'bulk' TiO_2 and TiO_2 particles, while Sunila (1988) demonstrate similar impacts due to cadmium, copper, lead, cobalt, iron and silver.

Bivalves' digestive gland has also been widely used for toxicity evaluation (Bignell et al., 2008; Marigómez et al., 2013) because it is the major organ involved in organism's homeostatic regulation, immune defence mechanisms and metabolism (Moore and Allen, 2002; Livingstone et al., 2006). The results obtained in the present study showed that rutile and anatase particles caused atrophy of this organ, which according to Cuevas et al. (2015) corresponds to a reduction in the thickness of epithelia followed by the expansion of the digestive tubule lumen. Rutile and anatase particles also caused hemocytes infiltration and accumulation of lipofuscin in digestive tubules. Previous studies also demonstrated that diamond nanoparticles (Cid et al., 2015), CdS quantum dots (Jimeno-Romero et al., 2019) and copper (Calabrese et al., 1984) induced similar histological alterations in bivalves' digestive gland.

Regarding mussel's biochemical changes, and in particular mussel's metabolism, the results obtained showed that the organisms metabolic capacity was not altered when exposed to rutile particles, which may indicate that the Ti concentrations tested under this form were not enough to impact mussels' metabolism. Other authors also demonstrated that low concentrations of mercury and carbon nanoparticles had no effects of mussel's metabolism (Coppola et al., 2017; Andrade et al., 2019). However, when mussels were exposed to anatase particles an increase on their metabolic capacity was observed, especially at the intermediate exposure concentration, showing that mussels exposed to this TiO_2 form were probably trying to prevent the effects of Ti, namely activating antioxidant and biotransformation defence mechanisms which requires higher metabolic capacity. Similarly, Monteiro et al. (2019) demonstrated that *M. galloprovincialis* exposed to high concentration of Ti (100 µg/L) increased their metabolic capacity. In this way, the present findings may indicate that although Ti concentrations were similar in mussels exposed to both TiO_2 forms, it seems that anatase can induce greater metabolic alterations than rutile. Thus, and in accordance to published studies and the present results, it seems that mussels' metabolic capacity may depend on the contaminant type and on the concentration tested, with higher concentrations exerting higher impacts.

Regarding mussels' energy reserves, the present study demonstrated that organisms were able to avoid the expenditure of GLY, regardless of the TiO_2 form. These results followed the ability of mussels to maintain their ETS activity when exposed to rutile particles, indicating that in stressful conditions mussels try to prevent the impacts by limiting their metabolic activity and saving GLY expenditure. The ability to maintain the ETS activity followed by the increased of GLY content was observed by Coppola et al. (2018) in *M. galloprovincialis* after exposure to arsenic. The results obtained further revealed that the increased metabolic capacity in mussels exposed to anatase particles was not high enough to lead to the expenditure of GLY. Once again, such results may highlight that the exposure concentrations tested were not high enough to lead to mussels' energy reserves expenditure or other energy reserves (such as lipids) were used to fuel up defence mechanisms. This pattern was also observed by Monteiro et al. (2019) in *M. galloprovincialis* after exposure to Ti. Nevertheless, in what regards to PROT content, this energy reserve decreased in mussels exposed to

Please cite this article as: C. Leite, F. Coppola, R. Monteiro et al., Biochemical and histopathological impacts of rutile and anatase (TiO_2 forms) in *Mytilus galloprovincialis*, Science of the Total Environment, https://doi.org/10.1016/j.scitotenv.2019.134886

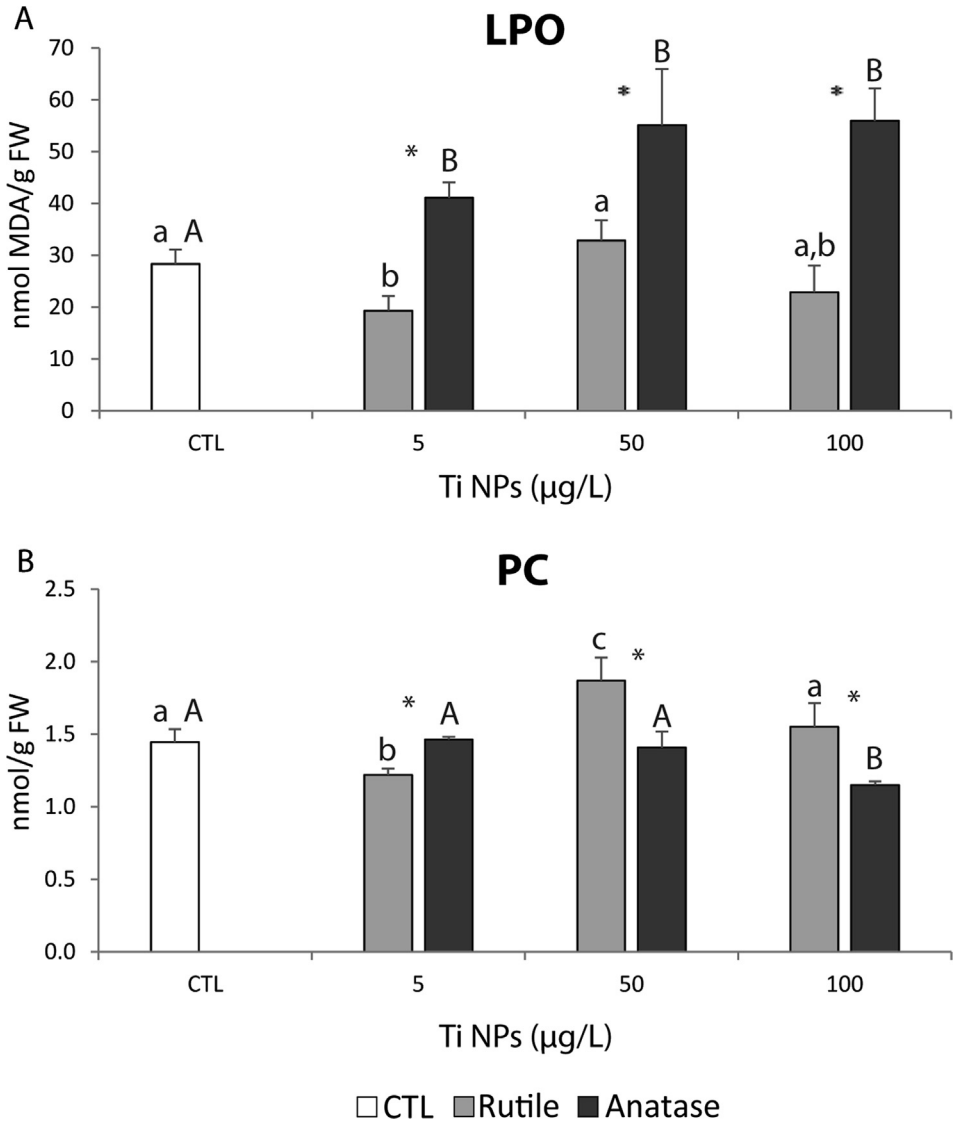

Fig. 8. A: Lipid peroxidation levels (LPO); and B: Protein carbonylation levels (PC), in *Mytilus galloprovincialis* exposed to different Ti concentrations of rutile and anatase. Results are mean + standard deviation. Significant differences ($p \leq 0.05$) among conditions are represented with different letters (lowercase letters for rutile; uppercase letters for anatase). Significant differences ($p \leq 0.05$) between the two forms of TiO_2 at each exposure concentration were represented with asterisks.

rutile and anatase particles, indicating that organisms were using proteins and were not able to increase their production under the exposure conditions, probably because the stress induced was not sufficient to activate the production of enzymes.

Under stressful conditions organisms, including mussels, normally increase the production of reactive oxygen species (ROS) and in order to avoid cellular damages they activate their antioxidant defences, including the activity of the enzymes superoxide dismutase (SOD), catalase (CAT), glutathione peroxidase (GPx) and glutathione reductase (GRed) (Regoli and Giuliani, 2014). Along with the activation of antioxidant defences, organisms exposed to stress conditions also activate biotransformation enzymes, namely glutathione S-transferases (GSTs) (Townsend and Tew, 2003; Sturve et al., 2008). Our findings suggest that the activity of antioxidant defences in mussels exposed to rutile particles, for most of the enzymes, did not increase with the increasing exposure concentration, corroborating the hypothesis that the conditions tested and/or the rutile reactivity were not sufficient to induce biochemical changes in mussels, namely increase on their antioxidant defences. Another possibility is that biotransformation defences, namely GSTs enzymes, were involved in cells detoxification from Ti, which was noticed at the highest exposure concentration and, for this reason, there was no need for antioxidant enzymes activation. The GSTs are an important group of enzymes whose function is catalyse the conjugation of a xenobiotic with glutathione (GSH) (Townsend and Tew, 2003) as well as inactivate lipid peroxidation products through the use of GSH as a reducing agent (Sturve et al., 2008). Previous studies demonstrated the non-activation of antioxidant enzymes while GSTs were activated, namely in *M. galloprovincialis* exposed to arsenic (Coppola et al., 2018) and in the same species exposed to silver nanoparticles (Ale et al., 2019). Nevertheless, in mussels exposed to anatase particles an opposite behaviour was detected. Mussels increased their antioxidant defences while decreasing the biotransformation defences (GSTs). These findings may result from the higher ROS production resulting from higher toxicity of anatase but also from the activation of mussel's metabolic capacity, assessed by the activity of ETS, since the mitochondrial transport system is one of the main ROS generators, leading to the activation of antioxidant enzymes. Again, this effect may be associated to the highest reactivity of anatase characteristic of its structure.

Please cite this article as: C. Leite, F. Coppola, R. Monteiro et al., Biochemical and histopathological impacts of rutile and anatase (TiO_2 forms) in *Mytilus galloprovincialis*, Science of the Total Environment, https://doi.org/10.1016/j.scitotenv.2019.134886

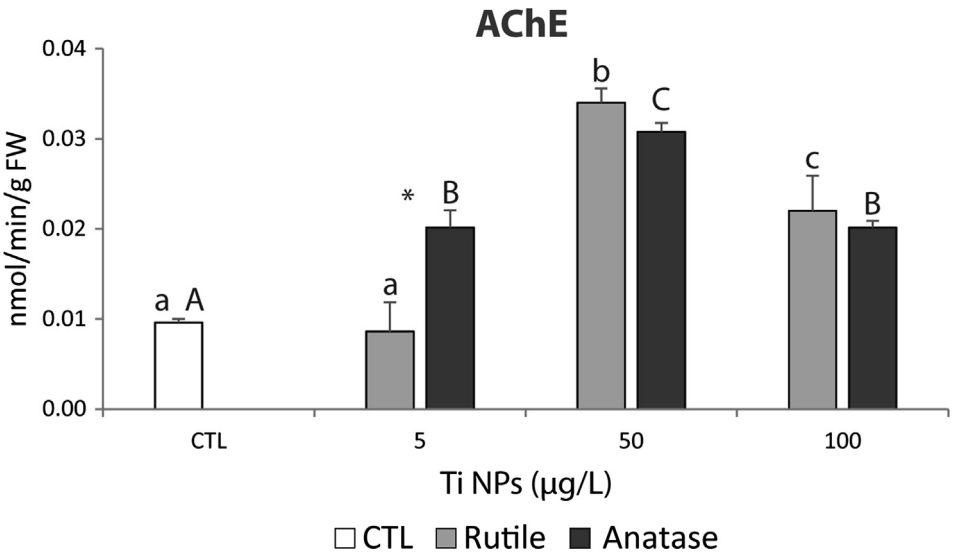

Fig. 9. Acetylcholinesterase activity (AChE), in *Mytilus galloprovincialis* exposed to different Ti concentrations of rutile and anatase. Results are mean + standard deviation. Significant differences ($p \leq 0.05$) among conditions are represented with different letters (lowercase letters for rutile; uppercase letters for anatase). Significant differences ($p \leq 0.05$) between the two forms of TiO_2 at each exposure concentration were represented with asterisks.

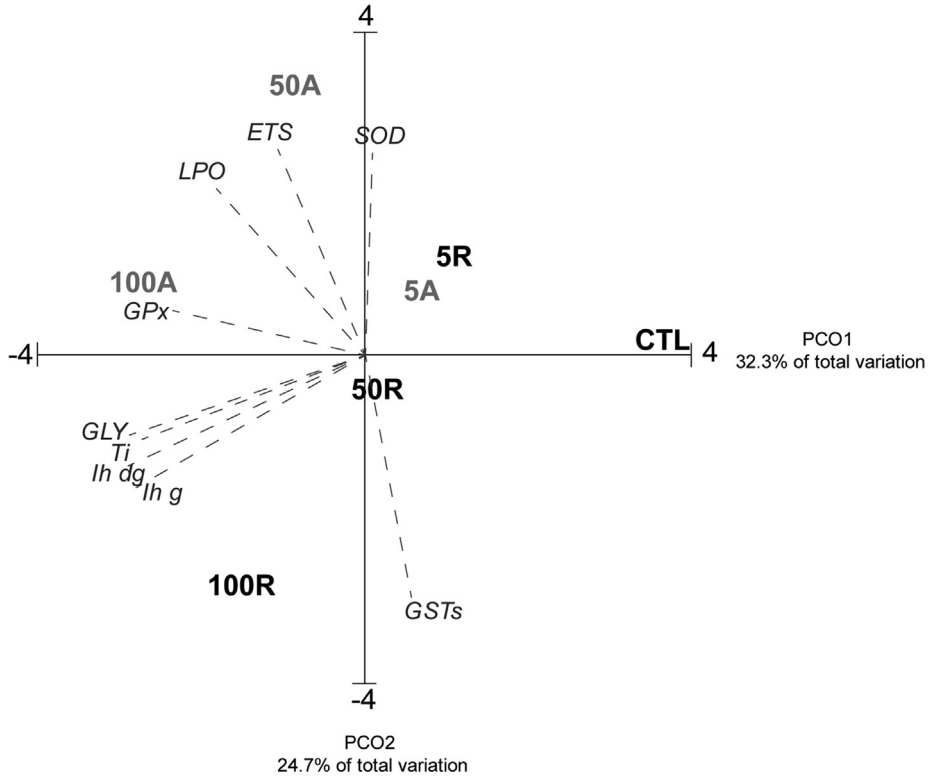

Fig. 10. Centroids ordination diagram (PCO) based on biochemical descriptors, histopathological indices and Ti concentration, measured in *Mytilus galloprovincialis* exposed to different Ti concentrations of rutile and anatase. Pearson correlation vectors are superimposed as supplementary variables ($r > 0.75$): Ti, IhG; IhDG; ETS; GLY; PROT; SOD; CAT; GPx; GRed; GSTs; LPO; PC; AChE.

As a consequence of low rutile toxicity, the results obtained revealed low cellular damages in mussels exposed to this TiO_2 form. Since antioxidant defences were not significantly activated, the present results highlight the low toxicity of rutile particles as well as the efficiency of the biotransformation defence system to detoxify rutile particles. Nonetheless, mussels exposed to anatase particles suffered cellular damages despite the increase in antioxidant defences. In this case, cellular damages may result from the excessive production of ROS and the inefficient ability of mussels to activate GSTs. Similarly, Andrade et al. (2019) also demonstrated that *M. galloprovincialis* exposed to carbon nanotubes lead to cellular damages and decreased in GSTs activity.

The present study further revealed that rutile and anatase particles induced neurotoxicity in mussels. The increased in AChE

activity is probably due to organisms' attempts to reduce neurotransmitter excess in the synaptic clefts. It has been reported that the increase on AChE activities reflected the neurotoxicity of TiO_2 particles in the scallop *Chlamys farreri* (Xia et al., 2017), which showed higher AChE values in contaminated organisms.

5. Conclusions

As conclusion, the present study showed that rutile and anatase particles were responsible for Ti bioaccumulation as well as biochemical and histopathological alterations in mussels, in a concentration-dependent way, with higher injuries identified in mussels exposed to higher Ti concentrations, regardless the TiO_2 form. These results are clearly highlighted by the PCO analysis, which separated organisms exposed to control conditions and the lowest Ti concentration for both rutile and anatase, from organisms exposed to higher concentrations. The mussels suffer the highest metabolic and oxidative stress impacts in the presence of anatase. These results are in agreement with several studies that already proved that anatase particles are more toxic than rutile particles (Braydich-Stolle et al., 2009; Zhang et al., 2013). The toxicity of anatase was mainly associated to low particle size. In particular, Zhang et al. (2013) demonstrated that the 25 nm anatase particles induced the strongest cytotoxicity and oxidative stress, followed by 5 and 100 nm anatase particles. In contrast, 100 nm rutile particles induced the lowest toxicity. In the present work, independently of the size of the TiO_2 particles as powders or even after dispersion in the exposure medium, within the duration of the study, the mussels were able to ingest similar quantities from both oxides for each initial concentration used. It was verified that the initial size of the particles should not be the most important parameter to explain the uptake of TiO_2. Despite the observation by SEM that anatase material was constituted by a more homogeneous mixture of particles with about 180 nm of size, while rutile was formed by a heterogeneous mixture of non-well-defined shaped particles with bigger sizes, both oxides were ingested by the mussels in similar amounts. Furthermore, as investigated by DLS the particles in suspension suffered aggregation phenomena, which lead to the deposition of larger aggregates. The smallest aggregates remained in suspension, available to the mussels, but with sizes significantly bigger than the particle sizes. From these observations, the toxicity of the TiO_2 particles to the mussels seems to be more related with the oxide nature than to the initial size of particles or aggregates. When comparing the two TiO_2 polymorphs, anatase particles induced higher injuries in mussels than rutile, especially in term of oxidative stress. This evidence is probably due to the metastability of the anatase crystallographic structure with tendency to adsorb radical species at the surface, which increase the cellular damage and promote the enhancement of the antioxidant defences. In agreement with this conclusion, Iswarya et al. (2016) demonstrated that anatase particles were more toxic than rutile, under visible irradiation in *Ceriodaphnia dubia*, and correlated the higher toxicity of anatase particles comparatively to rutile to the crystalline form and the aggregation of the particles.

Since both TiO_2 polymorphs induced histopathological changes compromising the physiological performance of *M. galloprovincialis*, this study highlights the risk of discharge TiO_2 even in low quantity into aquatic environment for the inhabiting organisms.

Declaration of Competing Interest

The authors declare that they have no known competing financial interests or personal relationships that could have appeared to influence the work reported in this paper.

Acknowledgments

Carla Leite benefited from BSc grant under the project ASARI-SAFE (NSFC/0001/2016) funded by the Portuguese Science Foundation (FCT). Francesca Coppola, and Rui Monteiro benefited from PhD grants (SFRH/BD/118582/2016 and SFRH/BD/108535/2015, respectively), given by the National Funds through the FCT, supported by FSE and Programa Operacional Capital Humano (POCH) e da União Europeia. Paula Ferreira acknowledge the grant IF/00300/2015. Rosa Freitas was funded by national funds (OE), through FCT, in the scope of the framework contract foreseen in the numbers 4, 5 and 6 of the article 23, of the Decree-Law 57/2016, of August 29, changed by Law 57/2017, of July 19. This work was also financially supported by the project BISPECIAl: BIvalveS under Polluted Environment and CIlmate chAnge PTDC/CTA-AMB/28425/2017 (POCI-01-0145-FEDER-028425) funded by FEDER, through COMPETE2020 - Programa Operacional Competitividade e Internacionalização (POCI), and by national funds (OE), through FCT/MCTES. Thanks are due for the financial support to CESAM (UID/AMB/50017/2019), CICECO (UID/CTM/50011/2019), CIIMAR (UID/Multi/04423/2019) and Smart Green Homes Project POCI-01-0247-FEDER-007678, financed by national funds through the FCT/MEC and when appropriate co-financed by FEDER under the PT2020 Partnership Agreement.

Appendix A. Supplementary data

Supplementary data to this article can be found online at https://doi.org/10.1016/j.scitotenv.2019.134886.

References

Ale, A., Liberatori, G., Vannuccini, M. L., Bergami, E., Ancora, S., Mariotti, G., Bianchi., N., Galdopórpora, J.M., Desimone, M.F., Cazenave, J., Corsi, I., 2019. Exposure to a nanosilver-enabled consumer product results in similar accumulation and toxicity of silver nanoparticles in the marine mussel Mytilus galloprovincialis. Aquat. Toxicol. 211, 46–56. http://doi.org/10.1016/j.aquatox.2019.03.018.

Allen, N.S., Edge, M., Verran, J., Caballero, L., Abrusci, C., Stratton, J., Maltby, J., Bygott, C., 2010. Photocatalytic surfaces: environmental benefits of Nanotitania. Open Mater. Sci. J. 3, 6–27. https://doi.org/10.2174/1874088X00903010006.

Almeida, Â., Freitas, R., Calisto, V., Esteves, V.I., Schneider, R.J., Soares, A.M.V.M., Figueira, E., 2015. Chronic toxicity of the antiepileptic carbamazepine on the clam *Ruditapes philippinarum*. Comp. Biochem. Physiol. C: Toxicol. Pharmacol. 172–173, 26–35. https://doi.org/10.1016/j.cbpc.2015.04.004.

Amachree, D., Moody, A.J., Handy, R.D., 2014. Comparison of intermittent and continuous exposures to inorganic mercury in the mussel, *Mytilus edulis*: Accumulation and sub-lethal physiological effects. Ecotoxicol. Environ. Saf. 109, 133–142. https://doi.org/10.1016/j.ecoenv.2014.07.025.

Amtout, A., Leonelli, R., 1995. Optical properties of rutile near its fundamental band gap. Phys. Rev. B 51 (11), 6842–6851. https://doi.org/10.1103/PhysRevB.51.6842.

Anderson, M.J., Gorley, R.N., Clarke, K.R., 2008. PERMANOVA+ for PRIMER: Guide to Software and Statistical Methods. PRIMER-E, Plymouth.

Andrade, M., De Marchi, L., Soares, A.M.V.M., Rocha, R.J.M., Figueira, E., Freitas, R., 2019. Are the effects induced by increased temperature enhanced in *Mytilus galloprovincialis* submitted to air exposure?. Sci. Total Environ. 647, 431–440. https://doi.org/10.1016/j.scitotenv.2018.07.293.

Au, D.W.T., 2004. The application of histo-cytopathological biomarkers in marine pollution monitoring: a review. Mar. Pollut. Bull. 48 (9–10), 817–834. https://doi.org/10.1016/j.marpolbul.2004.02.032.

Banni, M., Hajer, A., Sforzini, S., Oliveri, C., Boussetta, H., Viarengo, A., 2014. Transcriptional expression levels and biochemical markers of oxidative stress in *Mytilus galloprovincialis* exposed to nickel and heat stress. Comp. Biochem. Physiol. – C Toxicol. Pharmacol. 160 (1), 23–29. https://doi.org/10.1016/j.cbpc.2013.11.005.

Barbosa, J.S., Neto, D.M.A., Freire, R.M., Rocha, J.S., Fechine, L.M.U.D., Denardin, J.C., Valentini, A., de Araújo, T.G., Mazzetto, S.E., Fechine, P.B.A., 2018. Ultrafast sonochemistry-based approach to coat TiO_2 commercial particles for sunscreen formulation. Ultrason. Sonochem. 48, 340–348. https://doi.org/10.1016/j.ultsonch.2018.06.015.

Barmo, C., Ciacci, C., Canonico, B., Fabbri, R., Cortese, K., Balbi, T., Marcomini, A., Pojana, G., Gallo, G., Canesi, L., 2013. In vivo effects of n-TiO_2 on digestive gland and immune function of the marine bivalve *Mytilus galloprovincialis*. Aquat. Toxicol. 132–133, 9–18. https://doi.org/10.1016/j.aquatox.2013.01.014.

Beauchamp, C., Fridovich, I., 1971. Superoxide dismutase: improved assays and an assay applicable to acrylamide gels. Anal. Biochem. 44 (1), 276–287. https://doi.org/10.1016/0003-2697(71)90370-8.

Bernet, D., Schmidt, H., Meier, W., Wahli, T., 1999. Protoc. Bernet. 25–34. http://doi.org/10.1046/j.1365-2761.1999.00134.x.

Bignell, J.P., Dodge, M.J., Feist, S.W., Lyons, B., Martin, P.D., Taylor, N.G.H., Stone, D., Travalent, L., Stentiford, G.D., 2008. Mussel histopathology: effects of season, disease and species. Aquat. Biol. 2(1), 1–15. http://doi.org/10.3354/ab00031.

Bignell, J.P., Stentiford, G.D., Taylor, N.G.H., Lyons, B.P., 2011. Histopathology of mussels (Mytilus sp.) from the Tamar estuary, UK. Mar. Environ. Res. 72(1–2), 25–32. http://doi.org/10.1016/j.marenvres.2011.05.004.

Braydich-Stolle, L.K., Schaeublin, N.M., Murdock, R.C., Jiang, J., Biswas, P., Schlager, J. J., Hussain, S.M., 2009. Crystal structure mediates mode of cell death in TiO_2 nanotoxicity. J. Nanopart. Res. 11 (6), 1361–1374. https://doi.org/10.1007/s11051-008-9523-8.

Calabrese, A., MacInnes, J.R., Nelson, D.A., Greig, R.A., Yevich, P.P., 1984. Effects of long-term exposure to silver or copper on growth, bioaccumulation and histopathology in the blue mussel *Mytilus edulis*. Mar. Environ. Res. 11 (4), 253–274. https://doi.org/10.1016/0141-1136(84)90038-2.

Canesi, L., Ciacci, C., Fabbri, R., Marcomini, A., Pojana, G., Gallo, G., 2012. Bivalve molluscs as a unique target group for nanoparticle toxicity. Mar. Environ. Res. 76, 16–21. https://doi.org/10.1016/j.marenvres.2011.06.005.

Canesi, L., Fabbri, R., Gallo, G., Vallotto, D., Marcomini, A., Pojana, G., 2010. Biomarkers in *Mytilus galloprovincialis* exposed to suspensions of selected nanoparticles (Nano carbon black, C60 fullerene, Nano-TiO_2, Nano-SiO2). Aquat. Toxicol. 100 (2), 168–177. https://doi.org/10.1016/j.aquatox.2010.04.009.

Carlberg, I., Mannervik, B., 1985. Glutahione reductase. Methods Enzymol. 113, 484–490.

Carregosa, V., Figueira, E., Gil, A.M., Pereira, S., Pinto, J., Soares, A.M.V.M., Freitas, R., 2014. Tolerance of *Venerupis philippinarum* to salinity: osmotic and metabolic aspects. Comp. Biochem. Physiol. Mol. Integr. Physiol. 171, 36–43. https://doi.org/10.1016/j.cbpa.2014.02.009.

Cho, W.S., Kang, B.C., Lee, J.K., Jeong, J., Che, J.H., Seok, S.H., 2013. Comparative absorption, distribution, and excretion of titanium dioxide and zinc oxide nanoparticles after repeated oral administration. Part. Fibre Toxicol. 10 (1), 1. https://doi.org/10.1186/1743-8977-10-9.

Ciacci, C., Canonico, B., Bilaničová, D., Fabbri, R., Cortese, K., Gallo, G., Marcomini, A., Pojana, G., Canesi, L., 2012. Immunomodulation by different types of N-oxides in the hemocytes of the marine bivalve *Mytilus galloprovincialis*. PLoS One 7, (5). https://doi.org/10.1371/journal.pone.0036937 e36937.

Cid, A., Picado, A., Correia, J.B., Chaves, R., Silva, H., Caldeira, J., de Matos, A.P.A., Diniz, M.S., 2015. Oxidative stress and histological changes following exposure to diamond nanoparticles in the freshwater Asian clam *Corbicula fluminea* (Müller, 1774). J. Hazard. Mater. 284, 27–34. https://doi.org/10.1016/j.jhazmat.2014.10.055.

Coppola, F., Almeida, Â., Henriques, B., Soares, A.M.V.M., Figueira, E., Pereira, E., Freitas, R., 2017. Biochemical impacts of Hg in *Mytilus galloprovincialis* under present and predicted warming scenarios. Sci. Total Environ. 601–602, 1129–1138. https://doi.org/10.1016/j.scitotenv.2017.05.201.

Coppola, F., Almeida, Â., Henriques, B., Soares, A.M.V.M., Figueira, E., Pereira, E., Freitas, R., 2018. Biochemical responses and accumulation patterns of *Mytilus galloprovincialis* exposed to thermal stress and Arsenic contamination. Ecotoxicol. Environ. Saf. 147, 954–962. https://doi.org/10.1016/j.ecoenv.2017.09.051.

Costa, P.M., Carreira, S., Costa, M.H., Caeiro, S., 2013. Development of histopathological indices in a commercial marine bivalve (*Ruditapes decussatus*) to determine environmental quality. Aquat. Toxicol. 126, 442–454. https://doi.org/10.1016/j.aquatox.2012.08.013.

Cuevas, N., Zorita, I., Costa, P.M., Franco, J., Larreta, J., 2015. Development of histopathological indices in the digestive gland and gonad of mussels: integration with contamination levels and effects of confounding factors. Aquat. Toxicol. 162, 152–164. https://doi.org/10.1016/j.aquatox.2015.03.011.

D'Agata, A., Fasulo, S., Dallas, L.J., Fisher, A.S., Maisano, M., Readman, J.W., Jha, A.N., 2014. Enhanced toxicity of 'bulk'' titanium dioxide compared to ''fresh'' and ''aged'' nano-TiO_2 in marine mussels (*Mytilus galloprovincialis*). Nanotoxicology. 8 (5), 549–558. https://doi.org/10.3109/17435390.2013.807446.

Dame, R.F., 2008. Estuaries. Encyclopedia of Ecology, Vol. 2. Elsevier, Chichester, UK, pp. 484–490. https://doi.org/10.1016/B978-0-444-63768-0.00329-2.

D'Aniello, B., Polese, G., Luongo, L., Scandurra, A., Magliozzi, L., Aria, M., Pinelli, C., 2016. Neuroanatomical relationships between FMRFamide-immunoreactive components of the nervus terminalis and the topology of olfactory bulbs in teleost fish. Cell Tissue Res. 364 (1), 43–57. https://doi.org/10.1007/s00441-015-2295-4.

Dauvin, J.-C., Ruellet, T., 2009. The estuarine quality paradox: Is it possible to define an ecological quality status for specific modified and naturally stressed estuarine ecosystems?. Mar. Pollut. Bull. 59 (1–3), 38–47. https://doi.org/10.1016/j.marpolbul.2008.11.008.

De Coen, W., Janssen, C.R., 1997. The use of biomarkers in *Daphnia magna* toxicity testing. IV. Cellular Energy Allocation: a new methodology to assess the energy budget of toxicant-stressed Daphnia populations. J. Aquat. Ecosyst. Stress Recovery 6, 43–55. https://doi.org/10.1023/A:1008228517955.

de la Calle, I., Menta, M., Klein, M., Séby, F., 2017. Screening of TiO_2 and Au nanoparticles in cosmetics and determination of elemental impurities by multiple techniques (DLS, SP-ICP-MS, ICP-MS and ICP-OES). Talanta 171, 291–306. https://doi.org/10.1016/j.talanta.2017.05.002.

Dorier, M., Béal, D., Tisseyre, C., Marie-Desvergne, C., Dubosson, M., Barreau, F., Houdeau, E., Herlin-Boime, N., Rabilloud, T., Carriere, M., 2019. The food additive E171 and titanium dioxide nanoparticles indirectly alter the homeostasis of human intestinal epithelial cells in vitro. Environ. Sci. Nano 6 (5), 1549–1561. https://doi.org/10.1039/C8EN01188E.

Dubois, M., Gilles, K.A., Hamilton, J.K.J., Rebers, P.A., Smith, F., 1956. Colorimetric method for determination of sugars and related substances. Anal. Chem. 28 (3), 350–356. https://doi.org/10.1021/ac60111a017.

Ellman, G.L., Courtney, K.D., Andres, V., Featherstone, R.M., 1961. A new and rapid colorimetric determination of acetylcholinesterase activity. Biochem. Pharmacol. 7 (2), 88–95. https://doi.org/10.1016/0006-2952(61)90145-9.

Evans, D.H., 1987. The fish gill: site of action and model for toxic effects of environmental pollutants. Environ. Health Perspect. 71 (8), 47–58. https://doi.org/10.1289/ehp.877147.

Fadeel, B., Garcia-Bennett, A.E., 2010. Better safe than sorry: Understanding the toxicological properties of inorganic nanoparticles manufactured for biomedical applications. Adv. Drug Deliv. Rev. 62 (3), 362–374. https://doi.org/10.1016/j.addr.2009.11.008.

Gabe, M., 1968. Metachromacity of products of secretion rich in cystine after oxidation by certain peracids. C. R. Acad. Sci. Hebd. Seances Acad. Sci. D 267, 666–668.

Gong, X.-Q., Selloni, A., 2007. First-principles study of the structures and energetics of stoichiometric brookite TiO_2 surfaces. Phys. Rev. B 76, (23). https://doi.org/10.1103/PhysRevB.76.235307 235307.

Gottschalk, F., Nowack, B., 2011. The release of engineered nanomaterials to the environment. J. Environ. Monit. 13 (5), 1145–1155. https://doi.org/10.1039/c0em00547a.

Grätzel, M., 2001. Photoelectrochemical cells. Nature 414 (6861), 338–344. https://doi.org/10.1038/35104607.

Habig, W.H., Pabst, M.J., Jakoby, W.B., 1974. Glutathione S-transferases. The fist enzymatic step in mercapturic acid formation. J. Biol. Chem. 249 (22), 7130–7139.

Hanaor, D.A.H., Sorrell, C.C., 2011. Review of the anatase to rutile phase transformation. J. Mater. Sci. 46, 855–874.

Islam, M.S., Tanaka, M., 2004. Impacts of pollution on coastal and marine ecosystems including coastal and marine fisheries and approach for management: a review and synthesis. Mar. Pollut. Bull. 48 (7–8), 624–649. https://doi.org/10.1016/j.marpolbul.2003.12.004.

Iswarya, V., Bhuvaneshwari, M., Alex, S.A., Iyer, S., Chaudhuri, G., Chandrasekaran, P. T., Bhalerao, G.M., Chakravarty, S., Raichur, A.M., Chandrasekaran, N., Mukherjee, A., 2015. Combined toxicity of two crystalline phases (anatase and rutile) of Titania nanoparticles towards freshwater microalgae: Chlorella sp. Aquat. Toxicol. 161, 154–169. https://doi.org/10.1016/j.aquatox.2015.02.006.

Iswarya, V., Bhuvaneshwari, M., Chandrasekaran, N., Mukherjee, A., 2016. Individual and binary toxicity of anatase and rutile nanoparticles towards *Ceriodaphnia dubia*. Aquat. Toxicol. 178, 209–221. https://doi.org/10.1016/j.aquatox.2016.08.007.

Iswarya, V., Bhuvaneshwari, M., Chandrasekaran, N., Mukherjee, A., 2018. Trophic transfer potential of two different crystalline phases of TiO_2 Particles from Chlorella sp. to *Ceriodaphnia dubia*. Aquat. Toxicol. 197, 89–97. https://doi.org/10.1016/j.aquatox.2018.02.003.

Iswarya, V., Palanivel, A., Chandrasekaran, N., Mukherjee, A., 2019. Toxic effect of different types of titanium dioxide nanoparticles on *Ceriodaphnia dubia* in a freshwater system. Environ. Sci. Pollut. Res. 26 (12), 11998–12013. https://doi.org/10.1007/s11356-019-04652-x.

Jin, C., Tang, Y., Yang, F.G., Li, X.L., Xu, S., Fan, X.Y., Huang, Y.Y., Yang, Y.J., 2011. Cellular toxicity of TiO_2 nanoparticles in Anatase and Rutile crystal phase. Biol. Trace Elem. Res. 141, 3–15. https://doi.org/10.1007/s12011-010-8707-0.

Jiang, J., Oberdörster, G., Biswas, P., 2009. Characterization of size, surface charge, and agglomeration state of nanoparticle dispersions for toxicological studies. J. Nanopart. Res. 11 (1), 77–89. https://doi.org/10.1007/s11051-008-9446-4.

Jimeno-Romero, A., Bilbao, E., Valsami-Jones, E., Cajaraville, M.P., Soto, M., Marigómez, I., 2019. Bioaccumulation, tissue and cell distribution, biomarkers and toxicopathic effects of CdS quantum dots in mussels, *Mytilus galloprovincialis*. Ecotoxicol. Environ. Saf. 167, 288–300. https://doi.org/10.1016/j.ecoenv.2018.10.035.

Johansson, L.H., Håkan Borg, L.A., 1988. A spectrophotometric method for determination of catalase activity in small tissue samples. Anal. Biochem. 174 (1), 331–336. https://doi.org/10.1016/0003-2697(88)90554-4.

Kaegi, R., Ulrich, A., Sinnet, B., Vonbank, R., Wichser, A., Zuleeg, S., Simmler, H., Brunner, S., Vonmont, H., Burkhardt, M., Boller, M., 2008. Synthetic TiO_2 nanoparticle emission from exterior facades into the aquatic environment. Environ. Pollut. 156 (2), 233–239. https://doi.org/10.1016/j.envpol.2008.08.004.

Kennedy, V.C., Zellweger, G.W., Jones, B.F., 1974. Filter pore-size effects on the analysis of Al, Fe, Mn, and Ti in water. Water Resour. Res. 10 (4), 785–790. https://doi.org/10.1029/WR010i004p00785.

King, F.D., Packard, T.T., 1975. Respiration and the activity of the respiratory electron transport system in marine zooplankton. Limnol. Oceanogr. 20, 849–854.

Kiser, M.A., Westerhoff, P., Benn, T., Wang, Y., Pérez-Rivera, J., Hristovski, K., 2009. Titanium nanomaterial removal and release from wastewater treatment plants. Environ. Sci. Technol. 43 (17), 6757–6763. https://doi.org/10.1021/es901102n.

Leong, H.J., Oh, S.-G., 2018. Preparation of antibacterial TiO_2 particles by hybridization with azelaic acid for applications in cosmetics. J. Ind. Eng. Chem. 66, 242–247. https://doi.org/10.1016/j.jiec.2018.05.035.

Please cite this article as: C. Leite, F. Coppola, R. Monteiro et al., Biochemical and histopathological impacts of rutile and anatase (TiO_2 forms) in *Mytilus galloprovincialis*, Science of the Total Environment, https://doi.org/10.1016/j.scitotenv.2019.134886

Livingstone, D.R., Martinez, P.G., Michel, X., Narbonne, J.F., O'Hara, S., Ribera, D., Winston, G.W., 2006. Oxyradical production as a pollution-mediated mechanism of toxicity in the common mussel, Mytilus edulis L., and other molluscs. Funct. Ecol. 4 (3), 415. https://doi.org/10.2307/2389604.

Marigómez, I., Garmendia, L., Soto, M., Orbea, A., Izagirre, U., Cajaraville, M.P., 2013. Marine ecosystem health status assessment through integrative biomarker indices: a comparative study after the Prestige oil spill "mussel Watch". Ecotoxicology 22 (3), 486–505. https://doi.org/10.1007/s10646-013-1042-4.

Menard, A., Drobne, D., Jemec, A., 2011. Ecotoxicity of nanosized TiO_2. Review of in vivo data. Environ. Pollut. 159 (3), 677–684. https://doi.org/10.1016/j.envpol.2010.11.027.

Mennillo, E., Casu, V., Tardelli, F., De Marchi, L., Freitas, R., Pretti, C., 2017. Suitability of cholinesterase of polychaete Diopatra neapolitana as biomarker of exposure to pesticides: in vitro characterization. Comp. Biochem. Physiol. – C: Toxicol. Pharmacol. 191, 152–159. https://doi.org/10.1016/j.cbpc.2016.10.007.

Mesquita, C.S., Oliveira, R., Bento, F., Geraldo, D., Rodrigues, J.V., Marcos, J.C., 2014. Simplified 2,4-dinitrophenylhydrazine spectrophotometric assay for quantification of carbonyls in oxidized proteins. Anal. Biochem. 458, 69–71. https://doi.org/10.1016/j.ab.2014.04.034.

Mezni, A., Alghool, S., Sellami, B., Ben Saber, N., Altalhi, T., 2018. Titanium dioxide nanoparticles: synthesis, characterisations and aquatic ecotoxicity effects. Chem. Ecol. 34 (3), 288–299. https://doi.org/10.1080/02757540.2017.1420178.

Middlemas, S., Fang, Z.Z., Fan, P., 2013. A new method for production of titanium dioxide pigment. Hydrometallurgy 131–132, 107–113. https://doi.org/10.1016/j.hydromet.2012.11.002.

Mogilevsky, G., Chen, Q., Kleinhammes, A., Wu, Y., 2008. The structure of multilayered titania nanotubes based on delaminated anatase. Chem. Phys. Lett. 460 (4–6), 517–520. https://doi.org/10.1016/j.cplett.2008.06.063.

Monteiro, R., Costa, S., Coppola, F., Freitas, R., Vale, C., Pereira, E., 2019. Toxicity beyond accumulation of Titanium after exposure of *Mytilus galloprovincialis* to spiked seawater. Environ. Pollut. 244, 845–854. https://doi.org/10.1016/j.envpol.2018.10.035.

Moore, M.N., Allen, J.I., 2002. A computational model of the digestive gland epithelial cell of marine mussels and its simulated responses to oil-derived aromatic hydrocarbons. Mar. Environ. Res. 54 (3–5), 579–584. https://doi.org/10.1016/S0141-1136(02)00166-6.

Nowack, B., Ranville, J.F., Diamond, S., Gallego-Urrea, J.A., Metcalfe, C., Rose, J., Horne, N., Koelmans, A.A., Klaine, S.J., 2012. Potential scenarios for nanomaterial release and subsequent alteration in the environment. Environ. Toxicol. Chem. 31 (1), 50–59. https://doi.org/10.1002/etc.726.

Ohkawa, H., Ohishi, N., Yagi, K., 1979. Assay for lipid peroxides in animal tissues by thiobarbituric acid reaction. Anal. Biochem. 95 (2), 351–358. https://doi.org/10.1016/0003-2697(79)90738-3.

Pagano, M., Capillo, G., Sanfilippo, M., Palato, S., Trischitta, F., Manganaro, A., Faggio, C., 2016. Evaluation of functionality and biological responses of *Mytilus galloprovincialis* after exposure to quaternium-15 (Methenamine 3-Chloroallylochloride). Molecules 21 (2), 1–12. https://doi.org/10.3390/molecules21020144.

Paglia, D.E., Valentine, W.N., 1967. Studies on the quantitative and qualitative characterization of erythrocyte glutathione peroxidase. J. Lab. Clin. Med 70 (1), 158–169.

Paz, Y., 2010. Application of TiO_2 photocatalysis for air treatment: patents' overview. Appl. Catal. B 99 (3–4), 448–460. https://doi.org/10.1016/j.apcatb.2010.05.011.

Pinto, J., Costa, M., Leite, C., Borges, C., Coppola, F., Henriques, B., Monteiro, R., Russo, T., Di Cosmo, A., Soares, A.M.V.M., Polese, G., Pereira, E., Freitas, R., 2019. Ecotoxicological effects of lanthanum in *Mytilus galloprovincialis*: biochemical and histopathological impacts. Aquat. Toxicol. 211, 181–192. https://doi.org/10.1016/j.aquatox.2019.03.017.

Polese, G., Bertapelle, C., Di Cosmo, A., 2016. Olfactory organ of *Octopus vulgaris*: morphology, plasticity, turnover and sensory characterization. Biol. Open 5 (5), 611–619. https://doi.org/10.1242/bio.017764.

Rajalakshmi, S., Mohandas, A., 2005. Copper-induced changes in tissue enzyme activity in a freshwater mussel. Ecotoxicol. Environ. Saf. 62 (1), 140–143. https://doi.org/10.1016/j.ecoenv.2005.01.003.

Regoli, F., Giuliani, M.E., 2014. Oxidative pathways of chemical toxicity and oxidative stress biomarkers in marine organisms. Mar. Environ. Res. 93, 106–117. https://doi.org/10.1016/j.marenvres.2013.07.006.

Robichaud, C.O., Uyar, A.E., Darby, M.R., Zucker, L.G., Wiesner, M.R., 2009. Estimates of Upper bounds and trends in Nano-TiO_2 production as a basis for exposure assessment. Environ. Sci. Technol. 43 (12), 4227–4233. https://doi.org/10.1021/es8032549.

Robinson, H., Hodgen, C., 1940. The biuret reaction in the determination of serum proteins: a study of the conditions necessary for the production of a stable color which bears a quantitative relationship to the protein concentration. J. Biol. Chem. 135 (9), 707. https://doi.org/10.1017/CBO9781107415324.004.

Shi, X., Li, Z., Chen, W., Qiang, L., Xia, J., Chen, M., Zhu, L., Alvarez, P.J.J., 2016. Fate of TiO_2 nanoparticles entering sewage treatment plants and bioaccumulation in fish in the receiving streams. NanoImpact 3–4, 96–103. https://doi.org/10.1016/j.impact.2016.09.002.

Skrabal, S.A., 2006. Dissolved titanium distributions in the Mid-Atlantic Bight. Mar. Chem. 102 (3–4), 218–229. https://doi.org/10.1016/j.marchem.2006.03.009.

Sturve, J., Almroth, B.C., Förlin, L., 2008. Oxidative stress in rainbow trout (*Oncorhynchus mykiss*) exposed to sewage treatment plant effluent. Ecotoxicol. Environ. Saf. 70 (3), 446–452. https://doi.org/10.1016/j.ecoenv.2007.12.004.

Sunila, I., 1988. Acute histological responses of the gill of the mussel, *Mytilus edulis*, to exposure by environmental pollutants. J. Invertebr. Pathol. 52 (1), 137–141. https://doi.org/10.1016/0022-2011(88)90112-7.

Townsend, D.M., Tew, K.D., 2003. The role of glutathione-S-transferase in anti-cancer drug resistance. Oncogene 22 (47), 7369–7375. https://doi.org/10.1038/sj.onc.1206940.

Viarengo, A., Dondero, F., Pampanin, D.M., Fabbri, R., Poggi, E., Malizia, M., Bolognesi, C., Perrone, E., Gollo, E., Cossa, G.P., 2007. A biomonitoring study assessing the residual biological effects of pollution caused by the HAVEN wreck on marine organisms in the Ligurian sea (Italy). Arch. Environ. Contam. Toxicol. 53 (4), 607–616. https://doi.org/10.1007/s00244-005-0209-2.

Wang, J., Zhou, G., Chen, C., Yu, H., Wang, T., Ma, Y., Jia, G., Gao, Y., Li, B., Sun, J., Li, Y., Jiao, F., Zhao, Y., Chai, Z., 2007. Acute toxicity and biodistribution of different sized titanium dioxide particles in mice after oral administration. Toxicol. Lett. 168 (2), 176–185. https://doi.org/10.1016/j.toxlet.2006.12.001.

Wang, W., Nicholas, S., Samuel, N., 1996. Kinetic determinations of trace element bioaccumulation in the mussel *Mytilus edulis*. Mar. Ecol. Prog. Ser. 140, 91–113.

Wang, Z., Li, Y., Chen, H., Fan, J., Wang, X., Ma, X., 2019. Correlation between the radius of acceptor ion and the dielectric properties of co-doped TiO_2 ceramics. Ceram. Int. 45 (12), 14625–14633. https://doi.org/10.1016/j.ceramint.2019.04.181.

Ward, J.E., Kach, D.J., 2009. Marine aggregates facilitate ingestion of nanoparticles by suspension-feeding bivalves. Mar. Environ. Res. 68 (137–142). https://doi.org/10.1016/j.marenvres.2009.05.002.

Xia, B., Zhu, L., Han, Q., Sun, X., Chen, B., Qu, K., 2017. Effects of TiO_2 nanoparticles at predicted environmental relevant concentration on the marine scallop *Chlamys farreri:* an integrated biomarker approach. Environ. Toxicol. Pharmacol. 50 (128–135). https://doi.org/10.1016/j.etap.2017.01.016.

Yan, L., Stallard, R.F., Key, R.M., Crerar, D.A., 1991. Trace metals and dissolved organic carbon in estuaries and offshore waters of New Jersey, USA. Geochim. Cosmochim. Acta 55 (12), 3647–3656. https://doi.org/10.1016/0016-7037(91)90062-A.

Yang, K., Xing, B., 2009. Sorption of phenanthrene by humic acid-coated nanosized TiO_2 and ZnO. Environ. Sci. Technol. 43 (6), 1845–1851. https://doi.org/10.1021/es802880m.

Yang, W.-E., Hsu, M.-L., Lin, M.-C., Chen, Z.-H., Chen, L.-K., Huang, H.-H., 2009. Nano/submicron-scale TiO_2 network on titanium surface for dental implant application. J. Alloys Compd. 479 (1–2), 642–647. https://doi.org/10.1016/j.jallcom.2009.01.021.

Yokoi, K., van den Berg, C.M.G., 1991. Determination of titanium in sea water using catalytic cathodic stripping voltammetry. Anal. Chim. Acta 245, 167–176. https://doi.org/10.1016/S0003-2670(00)80217-2.

Yuzer, B., Guida, M., Ciner, F., Aktan, B., Aydin, M.I., Meric, S., Selcuk, H., 2015. A multifaceted aggregation and toxicity assessment study of sol–gel-based TiO_2 nanoparticles during textile wastewater treatment. Desalin. Water Treat. 57 (11), 4966–4973. https://doi.org/10.1080/19443994.2014.1000387.

Zhang, J., Song, W., Guo, J., Zhang, J., Sun, Z., Li, L., Ding, F., Gao, M., 2013. Cytotoxicity of different sized TiO_2 nanoparticles in mouse macrophages. Toxicol. Ind. Health 29 (6), 523–533. https://doi.org/10.1177/0748233712442708.

Zhu, X., Zhou, J., Cai, Z., 2011. TiO_2 Nanoparticles in the marine environment: impact on the toxicity of tributyltin to abalone (*Haliotis diversicolor* supertexta) Embryos. Environ. Sci. Technol. 45 (8), 3753–3758. https://doi.org/10.1021/es103779h.

Zupo, V., Glaviano, F., Paolucci, M., Ruocco, N., Polese, G., Di Cosmo, A., Costantini, M., Mutalipassi, M., 2019. Roe enhancement of *Paracentrotus lividus*: nutritional effects of fresh and formulated diets. Aquacult Nutr. 25 (1), 26–38. https://doi.org/10.1111/anu.12826.

Please cite this article as: C. Leite, F. Coppola, R. Monteiro et al., Biochemical and histopathological impacts of rutile and anatase (TiO_2 forms) in *Mytilus galloprovincialis*, Science of the Total Environment, https://doi.org/10.1016/j.scitotenv.2019.134886